Norwegian Meteorological Institute

MET report

no. 19/2015
Climate

# Towards a better use of the precipitation radar data; a feasibility study

Jean-Marie Lepioufle

Norwegian Meteorological Institute

# MET report

| | |
|---|---|
| **Title:**<br>Towards a better use of the precipitation radar data; a feasibility study | **Date**<br>2015-06-12 |
| **Section:**<br>Section Climate data and spatial analysis – METklim | **Report no.**<br>no. 19/2015 |
| **Author(s):**<br>Jean-Marie Lepioufle | **Classification**<br>● Free ○ Restricted |
| **Client(s):**<br>NVE | **Client's reference**<br>[Client's reference] |


**Abstract**

Quantitative precipitation estimation (QPE) from weather radar is of great importance in hydrology, urban hydrology, landslide modelling, and infrastructure design, to mention just a few in the domain of water management. Limitations are the length of available QPE time series and sources of error. In spite of significant progress, the residual errors within QPE radar are still large. A solution to express the residual uncertainties in radar estimates is to generate an ensemble of precipitation fields.
Quantitative precipitation nowcasting (QPN) is an important area of research within hydrology where the major aim is to improve the accuracy and increase the useful lead time of flood and flash-flood warning systems
This study is initiated within the frames of the collaboration agreement between the Norwegian Water Resources and Energy Directorate (NVE) and Norwegian Meteorological Institute (MET) in order to improve the use of radar into hydrologic and landslide model.
The study has two objectives:
i- to do a preliminary assessment of the use of QPN for the case study of the 23$^{rd}$ of July 2011 over the area covered by the radar located at Hurum (Norway)
ii- to identify key issues which should be investigated further in order to establish an ensemble QPN
Further work can be focused on using longer timeseries of QPE radar at sub-daily time resolution.
More attention would have to be put on areas with no reference sensor such as mountainous areas. Physic-statistic model based on the physics of the radar will be of a great help for these cases.
Incorporating ensemble QPE into a hydrologic model or landslide model will enable to analyze the propagation of the uncertainties through chain models. The chain can first be applied for hindcasting and then for forecasting.



**Keywords**
Radar post-processing, radar nowcasting, ensemble radar, residual error modelling, geostatistics


Disiplinary signature

Responsible signature

# Table of contents

# List of figures

a kriged residual error with constant μ, $\sigma$, and L choose into the a posteriori distributions, Bottom-left: same as middle-right with others parameters μ, $\sigma$, and L choose into the a posteriori distributions. Bottom-right: one run of a Bayesian-based simulation based on non-constant μ following the a posteriori distribution, and constant $\sigma$, and L choose into the posteriori distributions. 52

# 1 Introduction

Quantitative precipitation estimation (QPE) from weather radar is of great importance in hydrology, urban hydrology, landslide modelling, and infrastructure design, to mention just a few in the domain of water management.

For design purposes, return period and more generally extreme analysis is of importance. Such analysis is often based on rain gauge data. They are used to estimate rainfall depths for given probabilities of exceedance. Extreme values are then fitted to distribution probability function such as the Generalized Extreme Value (GEV). Finally, the fitted distribution is used to calculate the rainfall depth for a given return period.
Generally, only rain gauge data are used to obtain statistics of extreme. However, the number of rain gauge records of short duration rainfall, i.e. within hourly, is sparse. Besides, the spatial density of rain gauge networks is often too low to obtain reliable statistics of extreme areal rainfall for sub-hourly durations.
The potential of utilizing weather radar data for extreme value analyses has been already illustrated in several papers: Durrans et al. (2002) estimated rainfall depth-area relationships for different exceedance frequencies by fitting a Gumbel distribution to annual radar rainfall maxima for durations of 1, 2 and 4 h using an 8-year data set, the largest area size being approximately 1300 km². Allen and DeGaetano (2005) estimated extreme areal precipitation depths for return periods of 2, 5 and 10 years using a 5-year data set of 24-h accumulated rainfall for New Jersey and North Carolina (United States) for area sizes up to 20,000 km². Lombardo et al. (2006) used radar data to estimate areal reduction factors for durations of 1 to 120 min and return periods of 2 to 50 years for area sizes ranging from 1 to 900 km².
At the Norwegian Meteorological Institute (MET), Dyrrdal, (2012) provided an overview of methods for the estimation of extremes in Norway. The author highlights the importance of taking into account the spatial distribution of the precipitation. Further, analysis of extreme short-term precipitation by Ødemark et al, (2012) highlighted the usefulness of using QPE radar.

One of the main benefits of weather radars is its very dense sampling of precipitating systems in time and space, facilitating real-time warning and nowcasting of severe weather which may have huge socio-economic impacts. Limitations are the length of available QPE time series and sources of error.

Using reflectivity to estimate precipitation is improving given the increasing space-time resolution gage observations and weather radars. However, the presence of sources of error requires careful design system and sophisticated data processing. Among other source of errors, one can have: beam shielding and the vertical profile of reflectivity (Joss and Waldvogel, 1990; Kitchen, 1995; Joss and Lee, 1995; Pellarin et al., 2002; German and Joss, 2002; Bellon et al., 2007), beam smoothing and post-detection integration (Zawadzki, 1982), variability in raindrop size distributions and related uncertainty in the relation between reflectivity and rain rate (Joss and Gori, 1978; Lee and Zawadzki, 2005), attenuation by water on the radome (Germann, 1999), attenuation in heavy rain and hail (Delrieu et al., 2000), and overestimation in hail (Austin, 1987).
At MET, the remote sensing department is continuously working on improving these sources of error. A state of the correction in 2012 can be found in Elo (2012).

In spite of significant progress, the residual errors are still large and need to be taken into account, in particular in the context of operational hydrogeological applications such as issuing landslide forecast, river runoff forecasts or flash flood and debris flow warnings.
As expressed in Germann et al. (2009): "*we may think of a probability density function (pdf) that describes the range of possible values in space and time for each radar estimate. One single pdf per pixel, however, is not sufficient as errors are correlated in space and time, and one would need a pdf conditional on the values in the neighbourhood, or alternatively the full error variance–covariance matrix, the dimension of which corresponds to the total number of pixels in space and time. In practice, neither the conditional pdf nor the full error covariance matrix can be directly used in present hydrological models.*"
A solution to express the residual uncertainties in radar estimates is to generate an ensemble of precipitation fields, (Krajewski et al., 1985 and Germann et al., 2009). Each ensemble member is a possible realization given the reflectivity measurements and knowledge on the radar error structure (Germann et al., 2006a; Lee et al., 2007). The original (deterministic) radar precipitation field is perturbed with a stochastic component, which has the correct space–time covariance structure as defined by the radar error covariance matrix. The advantage of the ensemble as opposed to more classical approaches is the simple interface with hydrology: each member can directly be fed into the hydrological model. Instead of running the hydrological model only once, we run it several times. We thus get an ensemble of possible hydrological outputs, the spread of which represents the sensitivity of the hydrological system to the uncertainty in the radar precipitation fields on input. The idea to express uncertainty by adding a stochastic component has already shown interesting results for radar precipitation nowcasting (i.e. forecast lead times of a few hours (0-3 hours)) by Seed (2003) and Bowler et al. (2006), and included in a hydrological context by Berenguer et al. (2005).

Quantitative precipitation forecasting (QPF) is an important area of research within hydrology where the major aim is to improve the accuracy and increase the useful lead time of flood and flash-flood warning systems. As said in Abdella et al. (2013): "*For the flood prediction of large catchments with areal extents in the order of several thousands of square kilometers and response times in the order of several hours to days, the large scale QPFs by Numerical Weather Prediction models are usually sufficient to at least assess general trends. However, their probability to fail gets higher when moving to prediction in small urban catchments. The smaller sizes of urban catchments combined with the fast and strong sensitivity of their responses to the variations of precipitation pose a challenge. A reasonable QPF in such catchments requires a precise estimation of the initial states which is normally only achieved by direct observation and high spatio-temporal forecast resolution. Even when this requirement is fulfilled, an acceptable QPF quality is achieved only for forecast lead times of a few hours (0-3 hours)*".

Quantitative Precipitation Nowcasting (QPN) approaches estimate a motion vector field over the entire radar coverage domain and have shown effectiveness in estimating the translation of a variety of precipitation pattern types (Germann and Zawadzki 2002). The use of a pdf to express the uncertainty in radar nowcasts was proposed in Germann and Zawadzki (2004). As a next step, from the pdf nowcasts one may calculate an ensemble which is in agreement with the individual pdfs of all pixels. A prerequisite of these stochastic nowcasting approaches is a rigorous study of the sources of uncertainty and their relative importance (e.g. Germann and Zawadzki, 2006).

Tight collaboration between the Norwegian Water Resources and Energy Directorate (NVE) and MET has been strengthen for the improvement of the use of radar into hydrologic and landslide model.

This study has two objectives:
i- to do a preliminary assessment of the use of QPN for the case study of the 23rd of July 2011 over the area covered by the radar located at Hurum (Norway)
ii- to identify key issues which should be investigated further in order to establish an ensemble QPN

The study hasn't been focused on correcting reflectivity but on a better estimation of the residual QPE error.

The report is organized as follows.
Section 2 describes the different datasets and the chosen event for our case study.
Section 3 shows the feasibility study of the Quantitative Precipitation Nowcasting.
Section 4 presents the temporal filling-in of minute precipitation radar
Section 5 shows the residual error estimation and the ensemble Quantitative Precipitation Estimation radar
In order to identify the key issues, every section got a discussion

# 2 Data and case study

## 2.1 Weather Radar

The study has been focused on the C-band radar located at Hurum. The radar has a 240km radius coverage. QPN and residual error estimation have been based on QPE. Reflectivity signal (*Z*) of the radar provided by the remote sensing department has been transformed into precipitation (*R*) using the Marshall expression $Z = aR^b$, where a=200 and b=1.6.

## 2.2 Daily precipitation from gauges

An 84 manual gauges network over Hurum radar coverage has been used (figure 1). Only daily manual gauges have been used in order to get a reasonable level of data quality. Automatic gauges provide relevant measurements. Unfortunately their quality control is still not perfect but anyway on improvement. In the following of the report, daily precipitation manual gauges may be written as RRNSDNUD.

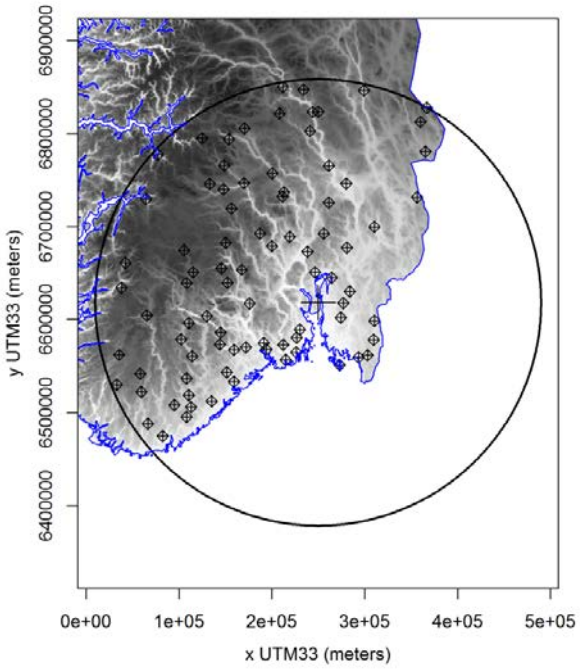


*Figure 1: The 84 manual gauges network within the Hurum radar coverage used in the study*

## 2.3 Case study: Hurum radar on the 23rd of July 2011

The whole study has been focused on the radar located at Hurum (figure 2) for one case study: the event that occurred on the 23rd of July 2011, an event that caused large destructions (figure 3).

It has been chosen because of its convective characteristic over the area. Figure 4 shows at around 17:00 a very low areal precipitation occurrence and a very high areal non zero precipitation areal mean. On this figure values are averaged over the Hurum radar coverage and thus might look low. In order to have an order of magnitude of the event we expressed the values over an area: the radar has measured at 17:00 a snapshot of 4524mm over an area of 120*120 km².

Among other places over the area, convective precipitation occurred over three municipalities: Fredrikstad, Oslo and Drammen. By taking Intensity/Duration/Frequency parameters from key gauges inside each municipality, and by computing return period using QPE over these three areas, one can have radar based return period values. For the three municipalities (Figure 5, 6 and 7) return periods reaches values higher than 200 years.

During this event, estimated precipitation from radar were recorded every 15 min. The current measure resolution at Hurum is now of 7.5min.

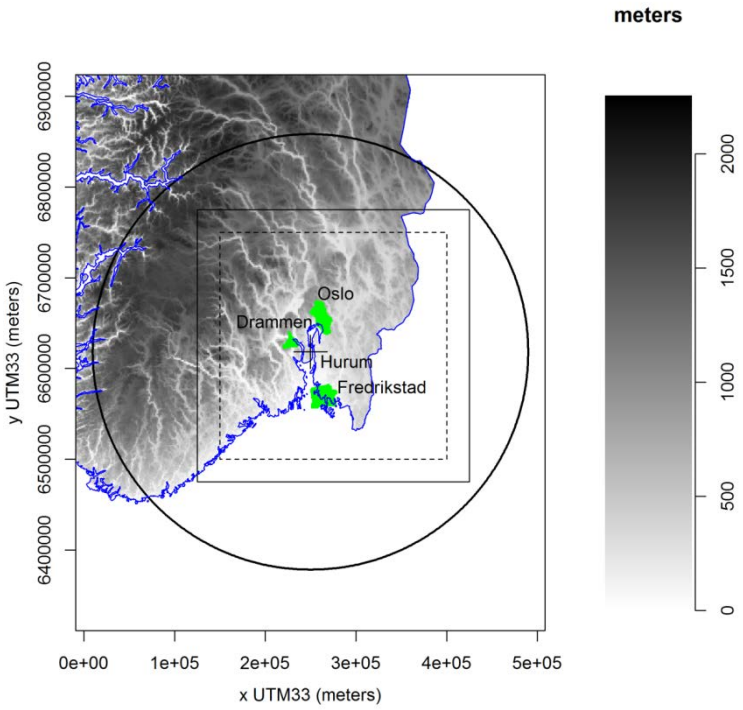


*Figure 2 Illustration of Hurum C-band radar coverage with a 240km radius. Green areas represent the three municipalities Fredrikstad, Oslo and Drammen. The larger square represents the area of study. The dashed square represents the area of advection detection in order to avoid border effect.*


*Figure 3 : consequence of the event in Notoden.*

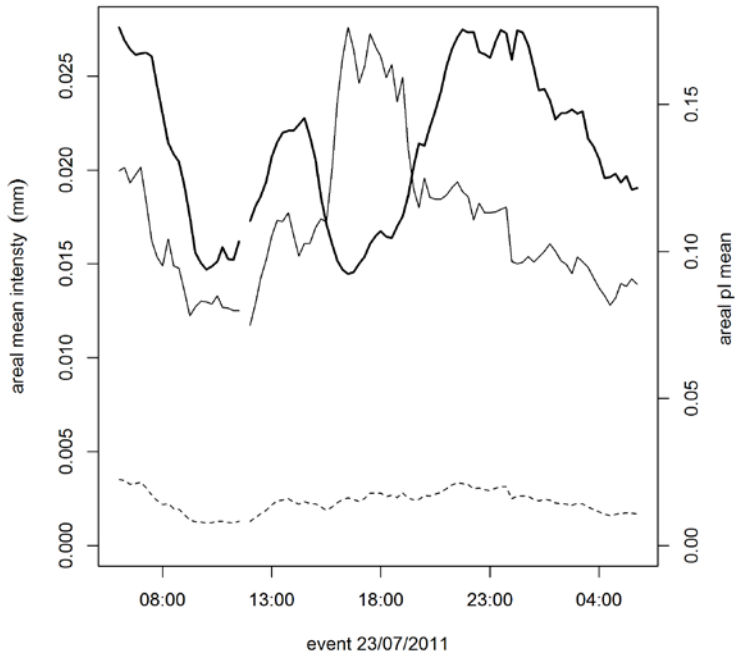


*Figure 4  Areal non-negative precipitation mean (line), areal mean precipitation occurrence (bold line), areal precipitation mean (dashed line)*

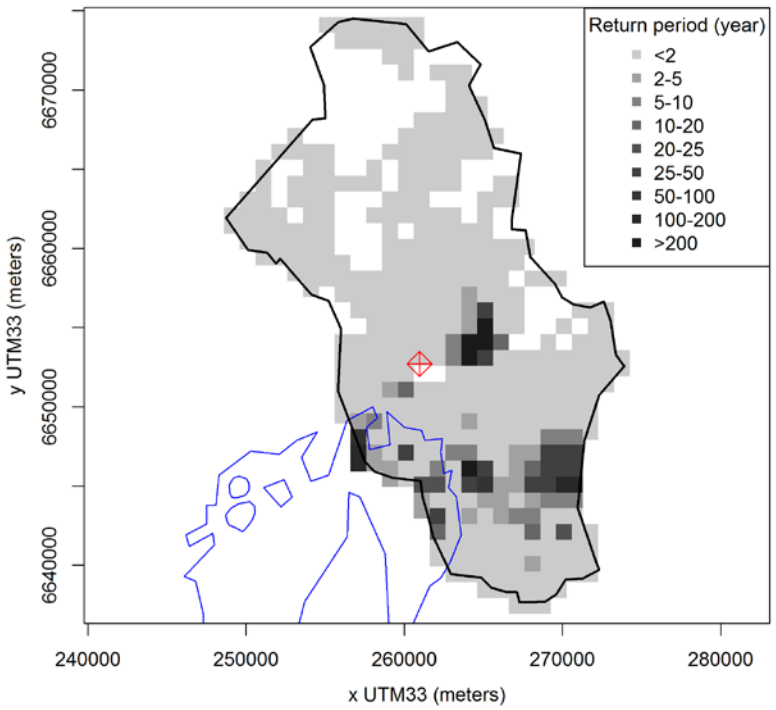


*Figure 5: return period, municipality of Oslo , based on the IDF parameters from station #18701 Oslo-Blindern illustrated in red*

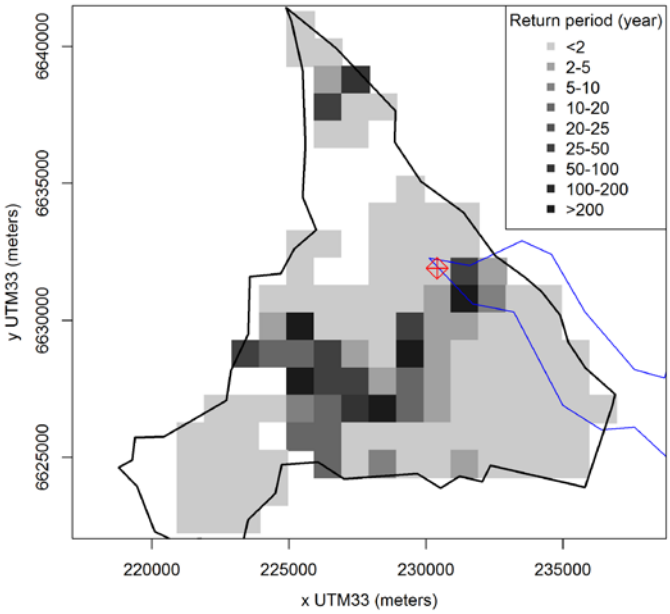


*Figure 6: Return period, Municipality of Drammen, based on the IDF parameters from station #26890 Drammen-Marienlyst illustrated in red*

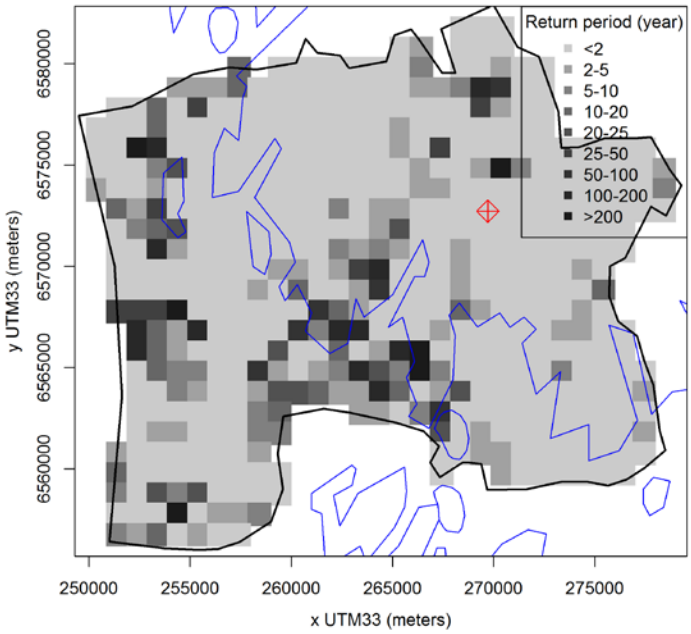


*Figure 7: Return period, Municipality of Fredrikstad, based on the IDF parameters from station #3030 Fredrikstad illustrated in red*

## 2.4 Discussion

It has been chosen to directly convert reflectivity into QPE using Marshall Expression with constant coefficient from literature. But the uncertainties in the $Z$−$R$ relationships when converting $Z$ into $R$ may introduce erroneous spatial patterns of precipitation. Ideally it would have been interesting to spend time on estimating spatially distributed parameters a and b. Or more practically, to use the Marshall expression very late in the study to keep reflectivity, direct measure of radar.

It was first decided to use hourly automatic gauges for QPE correction. Hourly precipitation or precipitation at higher time resolution such 10 min or minute is highly noisy. Regular methods based on Gaussian distribution are not relevant enough to qualify a value to be either an error or an extreme value. It is important then to know the characteristic of the phenomena that occurs on Norway or over a radar area at the time of the measure. The remote sensing department at MET developed a method to characterize the convectiveness or the stratiformness of an event. More information can be found in Yang et al. (2013). This method can be useful as an indicator of the process. Long time series are needed in order to train and thus infer the parameters of error models. Long time series of gauges are thus a necessity. Grouping similar precipitation phenomena into categories can be done by using neuronal network methods or self-organizing map method. These methods will sort, by themselves,

precipitation that looks more convective or stratiform. (Liu et al, 2011) Adapting these remarks with stochastic conditioned simulation will enable to highlight erroneous precipitation.
Besides of the noisy aspect of hourly (or 10 minute, 1 minute...) precipitation, measures are affected by wind and/or orography. No linear expression exists between precipitation, elevation and wind. An experimental site is established in order with the purpose to calibrate model of correction by using many sensors (Wolff et al., 2013). Results will definitely provide an idea of accurate correction to be established on this location. Unfortunately this site is representative for only one location. And effect of terrain and wind is highly changing from one location to another. Adding simplified physic model into the stochastic correction model would provide realism and thus be a great bonus.
An interesting aspect would be a more user oriented approach. One can first run a precipitation/hydrological chain model or a precipitation/landslide chain model using past event data. Spatial precipitation data are used as they are (either from radar or from spatial interpolation). The output values of the chain model are compared to past data. An error field is deduced from this difference. Precipitation fields are corrected according to this difference. The stochastic simulation will provide space-time realistic error fields.

Instead of automatic hourly gauge precipitation, it has been preferred to use manual daily gauges. Again, daily precipitation measures must be corrected. The method described in Førland et al. (1996) has been followed. The correction method takes into account temperature and the location of the gauges. Temperature is not always observed at the precipitation stations. Spatial interpolation of temperature has been established using the method and parameters described in Tveito et al (2000), Tveito et al. (2005) and Mohr (2008). The algorithms are summarized in Appendix 1. The temperature interpolation corresponds to the approach applied for SeNorge version 1.1. Parameters are based on averaged daily temperature over each month of the year in order to get the seasonality of the process. Unfortunately both orographic effect and daily fluctuation of the structure are not taken into account. The code has been developed in order to facilitate improvement of the correction. Ongoing work in part 1 of the NVE-MET common project is focused on improving the spatial temperature interpolation. Better temperature interpolation will enable more accurate precipitation correction especially at temperatures below 2 degrees.

So far, wind has not been applied for precipitation correction. Further work has to be done in providing wind map and to involve this field into the precipitation correction.

Precipitation, snow, temperature and wind must be consistent over time in order to not provide incoherent meteorological scenarios over time and space. It is thus important to create a weather generator that provides a temporal engine. The temporal engine provides a time series of categories whose to each category does correspond a probability of occurrence of one category of precipitation, one category of temperature, one category of… etc. The different categories related to each variable group the set parameters to be used for their interpolation or simulation.

The spatial return period presented in figures 4, 5 and 6 represent QPE values that have been expressed into return period by using only one gauge inside the area. These figures provide thus an order of magnitude of the event. A higher accuracy would be achieved by taking into account IDF parameters from several gauges. Several methods can be used for this. Spatial interpolation of point return period could provide a first idea of which parameters to be used on

the QPE. Stochastic simulation conditioned by gauges could provide long time series of realistic data in order to estimated IDF parameters on point with no measures. Other methods based on extreme simulation can be used as well.

# 3 Quantitative Precipitation Nowcasting

Nowcasting is defined as very short term forecast, with a lead time from 0 hour (now) to 2 hours. This study has focused on the feasibility of a simple nowcasting method, called Lagrangian persistence, to provide information relevant for NVE. The estimated precipitation has been assumed perfect in order to focus on the nowcasting method.

The method has been established and assessed on the event that occurred on the 23 of July 2011.

## 3.1 Lagrangian persistence nowcasting

The radar nowcasting method has been based on a frozen Lagrangian precipitation field, whose no dissipation would occur for the future next steps. For each time step t, an advection field has been detected from the precipitation field. The advection field has then been used for doing a rigid shift (figure 8) of the estimated precipitation to lead times from 15min to 3 hours. The advection stays unchanged for the whole nowcasting. The Lagrangian persistence nowcasting is summarized in the following expression:

$$R^*(t+\tau,\vec{x}) = R\left(t,\vec{x}-\vec{U}.\tau\right) \quad (3.1)$$

Where $R^*$ is the nowcasted precipitation field, $R$ is the observation field, $\vec{U}$ the advection field, $\vec{x}$ the location and $\tau$ the lead time of the nowcast.

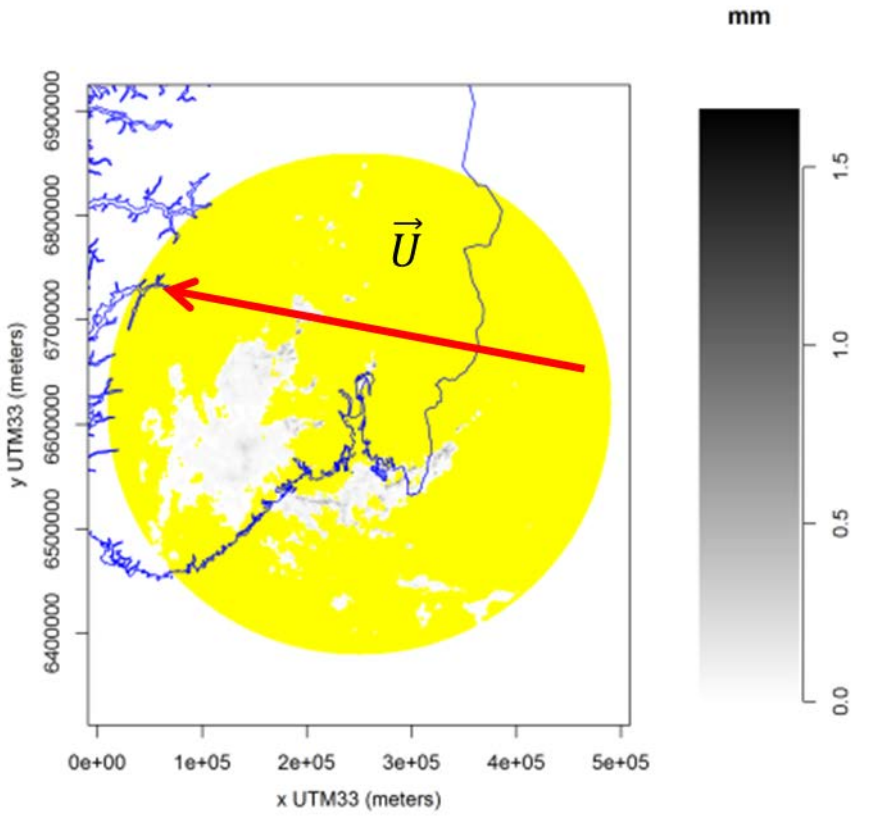


*Figure 8: Nowcasting method based on the translation of the QPE with a rigid global advection over the area represented on figure 2 (dashed square). Yellow area represents dry area under the Hurum radar coverage*

## 3.2 Advection detection

The advection (intensity and direction) has been detected using the non-zero precipitation values. It has been detected by using the field at time t and the field on the next time step. Either a global or a distributed advection over space can be detected. The advection field is determined by its minimization of the Relative Mean Square Error (RMSE) between the shifted field from time t to the next time step and the observed field at the next time. So far the distribution of the advection has been chosen Uniform. The code has been developed in order to let the possibility to add other distribution functions than uniform for a Bayesian detection of the advection. In the case of a detection of a distributed advection over space, a second estimation has been establish in order to estimate the spatially distributed noise to be added for minimizing the RMSE of the shifted field from time t to the next time step and the observed field at the next time step.

Another well-known method to detect advection is called cross-correlation method (Li, et al 1995). Nonetheless given the computing time for processing the method, the first one has been preferred.

## 3.3 Assessment and evaluation criteria

Comparison to observed estimated precipitation has been used to assess the simple nowcasting method (figure 9). Several scores exist such as correlation coefficient (CORR), probability of detection (POD), false alarm ratio (FAR), critical success index (CSI), equitable threat score (ETS) and the conditional mean absolute error (CMAE). They measure the agreement between the forecasts (F) and the observations (O) based on a pixel-to-pixel comparison. In the case of precipitation forecast the Stable Equitable Error in Probability Space score (SEEPS) (Rodwell et al. 2010) has been preferred. The SEEPS score is a combination of a 3 by 3 contingency table and a 3 by 3 weight table (figure 10). In the weight table the colour red means a high weight and the green colour a light weight. The distribution of the weight enables to disqualify method that makes wrong prediction in terms of precipitation occurrence and extreme precipitation amount. The lower the value, the better the forecast.

As expressed in Abdella et al. (2013): "*Another factor which adds to the overall reduction of [the score] values in this study is the high spatial resolution of the forecasts. The calculation of all the performance measures is based on pixel-to-pixel comparisons at the resolution of 1 km. The results in stricter evaluation with lower tolerance to errors made due to misplacement of predicted features. If a forecast at pixel level does not compare well with the available observation, it does not mean that the performance is poor. This is why some studies employ other evaluation methods, such as object-based methods, in addition the pixel-to-pixel verification (…). In order to analyse the effect of increasing tolerance to error due to misplacement, the [score] was calculated for an extended verification area surrounding a forecasted pixel. (…) When evaluation over an extended grid, each individual pixel is compared against all of the pixels located in the square region surrounding that pixel. For example, a 'hit' is registered if the forecast at the pixel of interest and the observation in one of the surrounding pixels both exceed the specified threshold.*"

The assessment has thus been done regarding three spatial supports:

- Every single nowcasted value has been compared to the observation at the same location.
- Every single nowcasted value has been compared to the value at the location that fits the best the prediction within an area of 9km² around the predicted location
- Every single nowcasted value has been compared to the value at the location that fits the best the prediction within an area of 25km² around the predicted location.

Figure 11 sums-up the three comparisons.

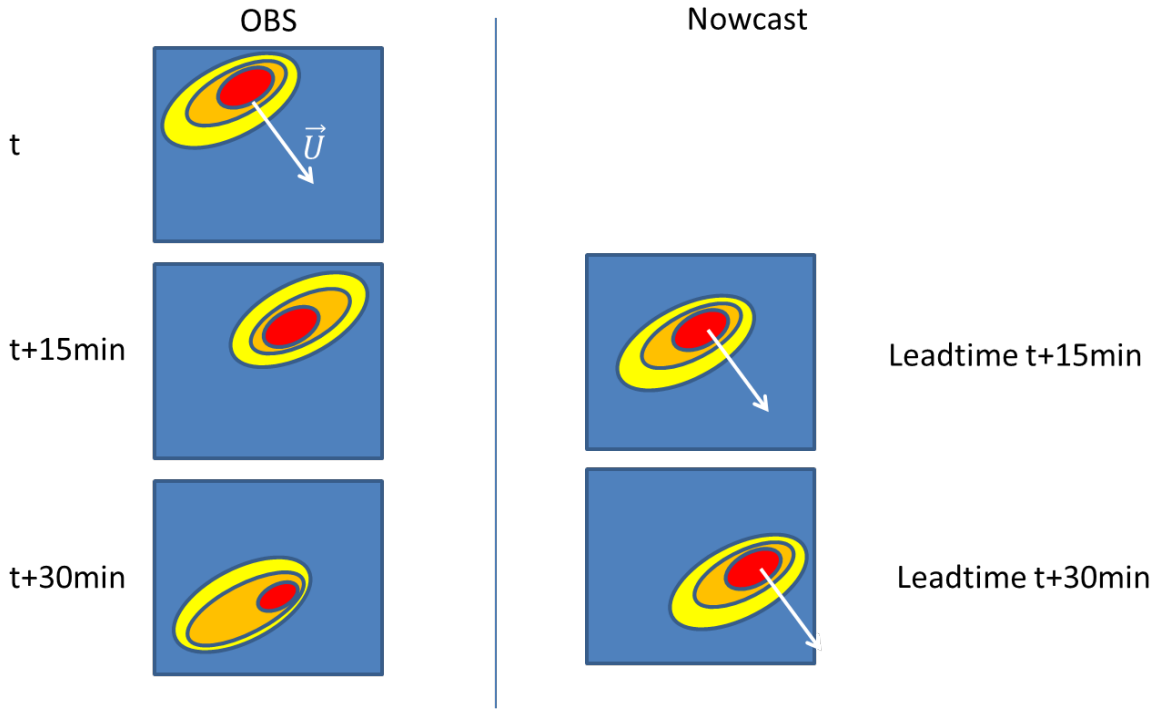


*Figure 9: Simple illustration of an observed estimated precipitation on the right, and the corresponding nowcasted precipitation at the different lead times on the left.*

Contingency table

OBSERVATION

| FORECAST | DRY | Light precip | Heavy precip |
|---|---|---|---|
| DRY | a | b | c |
| Light precip | d | e | f |
| Heavy precip | g | h | i |

Weight table

OBSERVATION

| FORECAST | DRY | Light precip | Heavy precip |
|---|---|---|---|
| DRY | | | |
| Light precip | | | |
| Heavy precip | | | |

*Figure 10: The SEEPS score (Rodwell et al. 2010) is a combination of a 3 by 3 contingency table and a 3 by 3 weight table. In the weight table the colour red means a high weight and the green colour a light weight. The distribution of the weight enables to disqualify method that makes wrong prediction in terms of precipitation occurrence and extreme precipitation amount.*

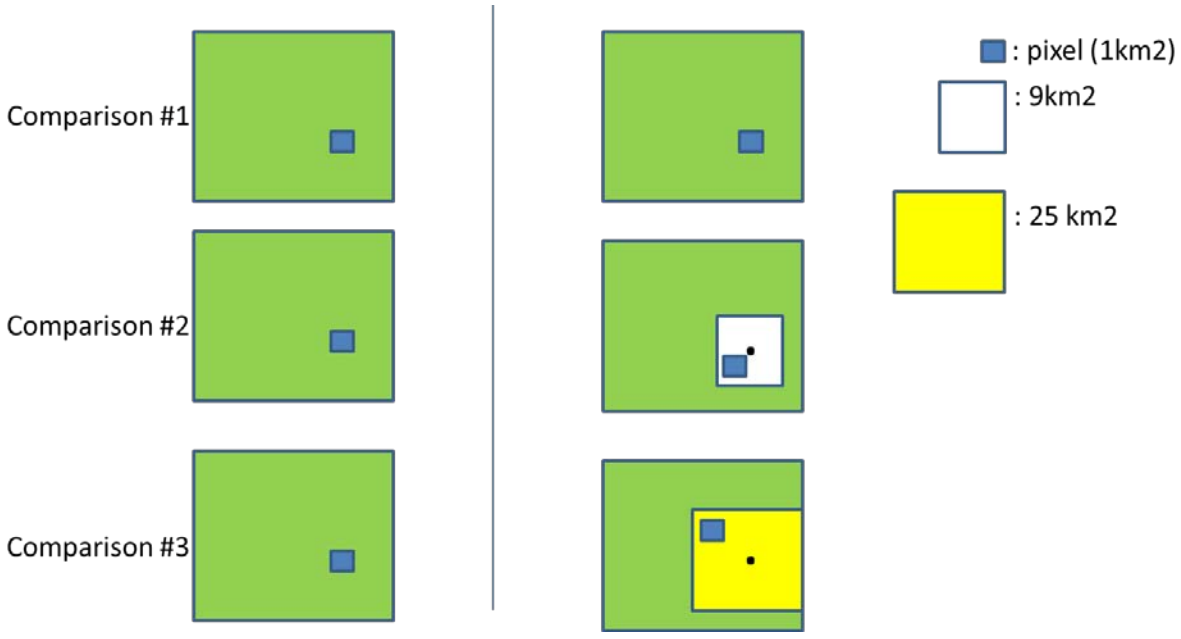


*Figure 11: Illustrative overview of the comparison methods…*

## 3.4 Results

Assessment of the radar nowcasting method for the event of the 23rd of July 2011 has been represented in figure 12. SEEP scores are represented for nowcasted precipitation for lead times going from 15min to 180min. The assessment regarding three spatial supports has been represented: the black curve represents the pixel to pixel comparison, the red curve represents the pixel to 9 km² comparison, and the green curve represents the pixel to 25 km². The larger the area of comparison, the lower SEEP. The left Y-axis has been used in order to catch the high value of the SEEP score of the black curve. It did comfort us that the used method is very simple and thus without any surprise did not manage to predict the small scales dissipation of precipitation. Nonetheless this method has been providing interesting and useful information over 9km²-areas. Indeed until two hours (120min) lead-time SEEP stand low enough (below 0.4).

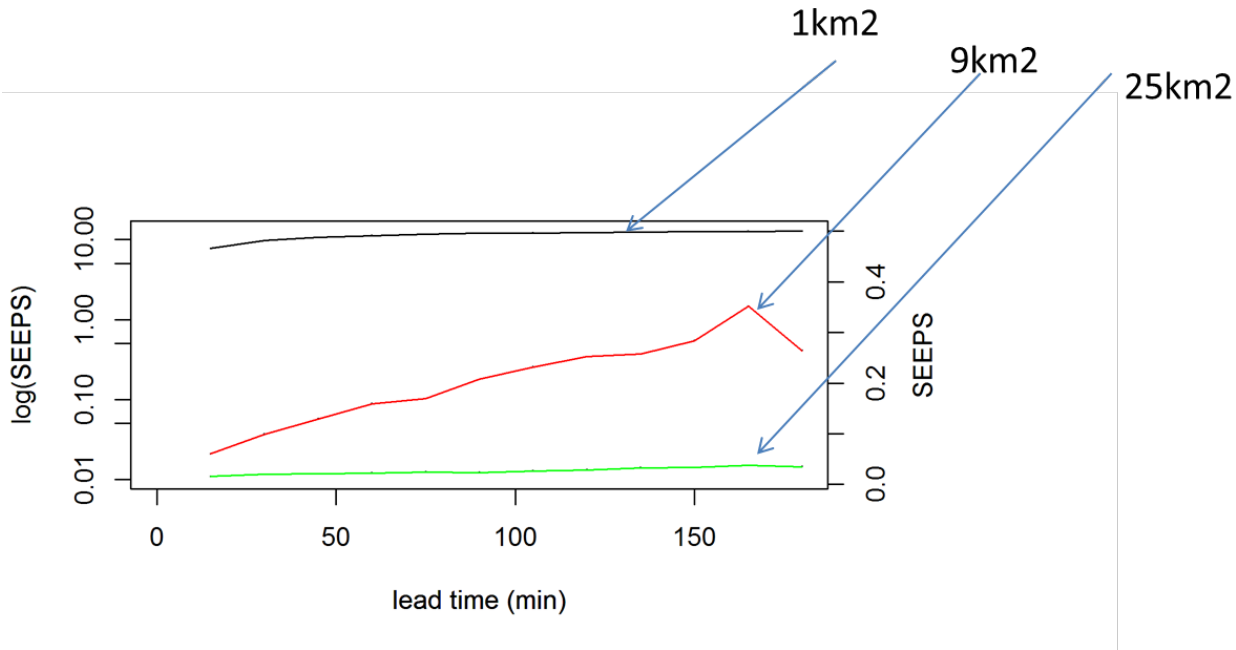


*Figure 12: SEEP score for nowcasted precipitation for lead times going from 15min to 180min. The three comparison are represented: the black curve represents the pixel to pixel comparison, the red curve represents the pixel to 9 km² comparison, the green curve represents the pixel to 25 km².*

## 3.5 Discussion

Assessment of the radar nowcasting method for the event of the 23rd of July 2011 has been represented in figure 12. A degradation of performance with lead time is obvious from the figures and is expected. The spatial resolution of the nowcast has an influence on the SEEPS score. The calculation of all the performance measures is based on pixel-to-pixel comparisons at the resolution of 1 km. The results in stricter evaluation with lower tolerance to errors made due to misplacement of predicted features. If a nowcast at pixel level does not compare well with the available observation, it does not mean that the performance is poor. In order to

analyse the effect of increasing tolerance to error due to misplacement, the SEEPS was calculated for an extended verification area surrounding a nowcasted pixel. The verification areas are square regions with side lengths ranging at 3 and 5 pixels. When evaluation over an extended grid, each individual pixel is compared against all of the pixels located in the square region surrounding that pixel (Abdella et al., 2013).
The results of the performance for larger verification area are presented in Figure 12. It illustrates the increase in nowcast skill, as quantified by SEEPS, as the verification area is increased from a single pixel (1 km2) up to a 5 x 5 pixel area.

In order to make a parallel to what MET and specifically yr.no provide to users, let us look at figure 13 and let us assume that the dark blue represent the one pixel value (1 km² spatial resolution) and the light the spatial uncertainty based on an a 9 km² area. So far the simple method does not enable to provide relevant information at the pixel resolution but enable to provide relevant spatial uncertainty information.

The QPN method used in this study has to be improved on several points:

1- The advection method:
Many researchers and institutes have been working on this topic. A simple google search enables to get an overview of the methods. The improvement would not face any problem. An important task will be to make advection having acceleration and an evolving direction. The topic is thus not precipitation nowcasting anymore but wind nowcasting.
Satellite data can be interesting to have prior information of the advection field. NWP can be helpful in order to get wind information at larger spatial resolution.

2- Growth and dissipation of precipitation:
The precipitation nowcasting method is based on a frozen precipitation field. It is obvious that temporal precipitation fluctuation occurs over time with as consequence growth or dissipation of the precipitation. Methods like dynamic Lagrangian kriging might provide proxies of the rainy area fluctuation over time. Conditional stochastic simulation would provide realistic space-time precipitation fluctuation within these wet areas. NWP might be interesting as well. Nonetheless, contrarily to remote sensing observation, NWP is a prediction with its own physics that might not match the meteorological event that is occurring.

3- Precipitation nowcasting for urban hydrology request a spatial resolution much higher than 1km². Challenge will be to know the need of the user, for example threshold values with accurate and narrow uncertainty, instead of trying to provide map of precise values with wide uncertainty.

4-Convective phenomena or orographic effect are the limit of a simple nowcasting method. A combination of strong machine learning, high level statistics and light physics based model is required. NWP might come later to make the transition between nowcasting and regular forecast.

Besides, this part of the study did assume QPE to be perfect. That is not the case in reality. The following of the report deal with estimating the residual error.

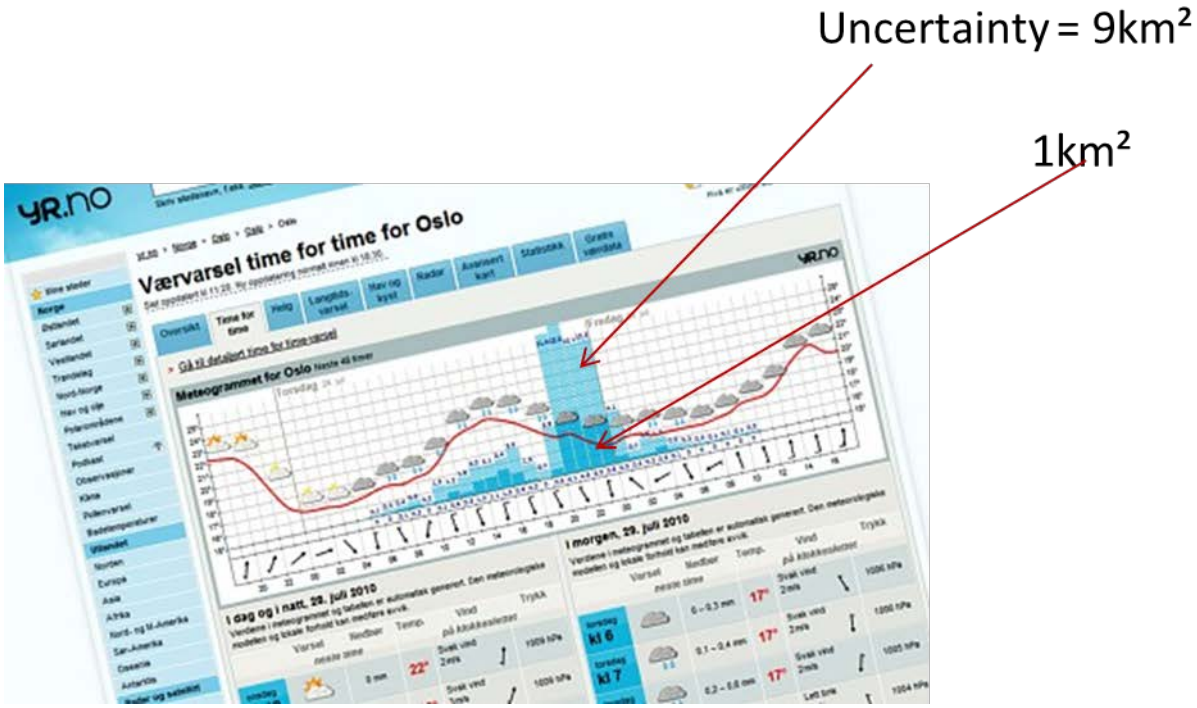


*Figure 13: Comparison and similitude to Yr forecast illustration.*

# 4 Temporal filling-in of minute precipitation radar

Radar observations are not continuous over time but discrete with a time resolution of 15 min for the event of the 23rd of July 2011 (7.5 min now). Quantitative Precipitation Estimation from radar (QPE) does not represent a temporal accumulation over 15 min. Indeed the frequency of measurement is different from the measure resolution. As a consequence zebra pattern appears when aggregating over time. Figure 14 is an illustration of the daily precipitation mean on the 23rd of July 2011. Whatever the correction or residual error estimation, zebra pattern will always occur. We assumed that estimated precipitation from radar to be a 1-min time resolution measurement. Filling-in the estimated precipitation between every 15 min time step enables to make the estimated precipitation field more realistic.

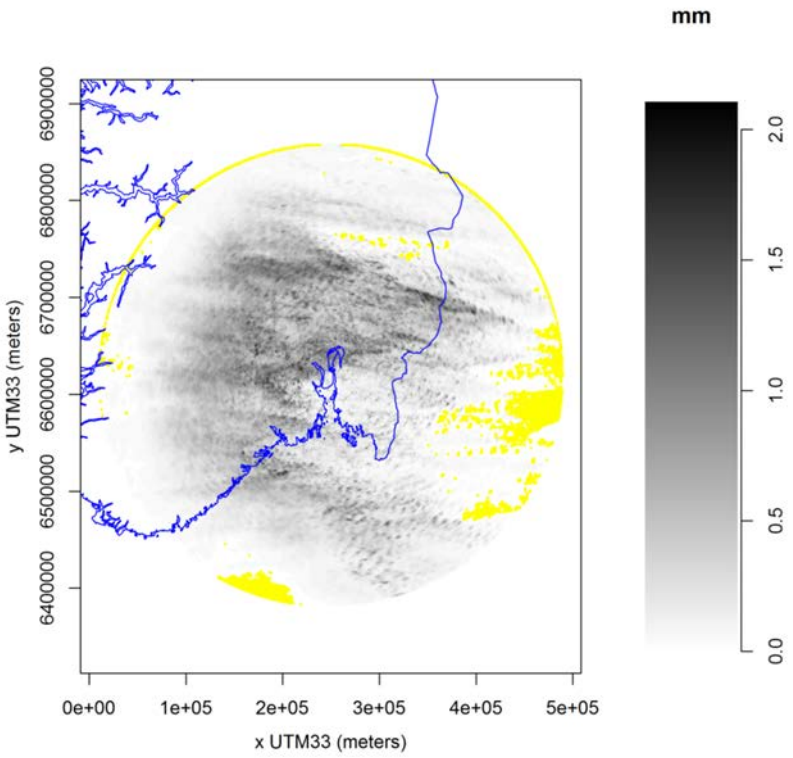


*Figure 14: Daily QPE mean*

## 4.1 Lagrangian linear interpolation

The Lagrangian approach enables a decomposition of the space-time dynamic of the precipitation into i-the advection and ii- the inner variability, also called fluctuation or dissipation. Several studies (i.e. Amani, et al., 1997) highlighted the importance of analysing precipitation fields in the Lagrangian reference in order to improve the accuracy of the geostatistics descriptors (spatial and temporal correlation distance).

We used the Lagrangian linear interpolation to fill-in the lack of information. The linear interpolation of each pixel is written:

$$R^*(t+\alpha.\Delta t,\vec{x}) = \alpha.R(t,\vec{x}) + (1-\alpha)R\left(t+\Delta t,\vec{x}-\vec{U}.\Delta t.\alpha\right), \alpha \in [0;1] \quad (4.1)$$

Where $R^*$ is the predicted precipitation field at time $t+\alpha.\Delta t$ and location $\vec{x}$, $R$ are the observation fields at location $(t,\vec{x})$ and $\left(t+\Delta t,\vec{x}-\vec{U}.\Delta t.\alpha\right)$ where $\vec{U}$ is the advection field.

It enables to provide quickly values at each minute time resolution.

The process of filling-in the QPE is as follow:

1-For every hour the spatially distributed advection is either provided by an external source or computed from the 1-min precipitation radar itself.

2-Hourly average of the distributed advection

3-Transcription of the 1-min estimated precipitation field from the Eulerian reference (the one we used to see measurement) to the Lagrangian reference by using the hourly advection.

4-Linear interpolation

5-Transcription of the estimated precipitation field from the Lagrangian reference to the Eulerian field

An algorithmic overview of the process is shown on figure 15.

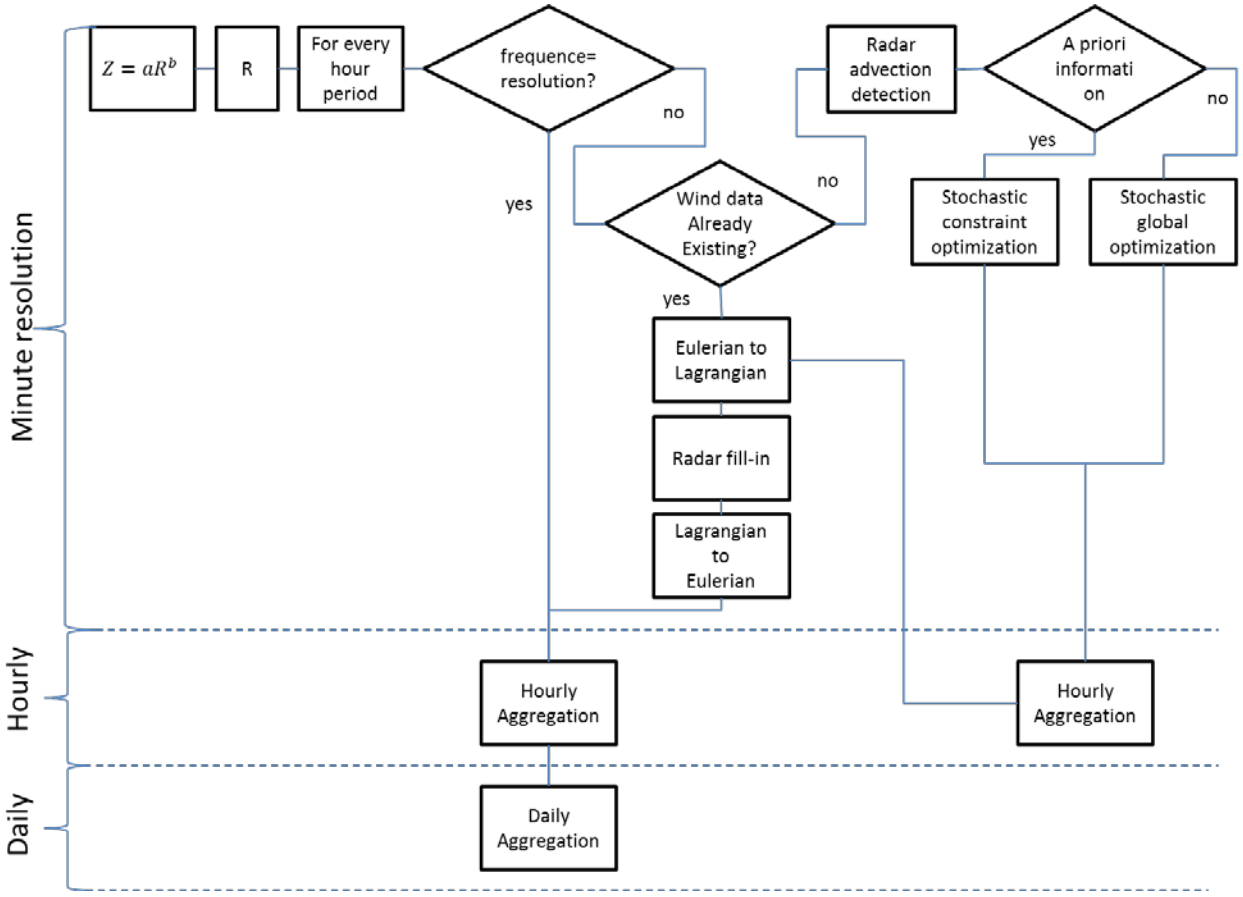


*Figure 15: Algorithmic overview of the filling-in method*

## 4.2 Results

As an illustration, advection fields and their corresponding precipitation fields are shown on figure 16. Figure 17 shows an hourly aggregated precipitation field on the 23rd of July 2011 from 07:00 to 07:59 after a filling-in. Figure 18 shows the daily aggregated precipitation on the 23rd of July 2011.

As an illustration of the improvement, one can see that amount of daily precipitation goes from a maximum of 2mm before filling-in (figure14) to a maximum of 25 mm in figure 18.

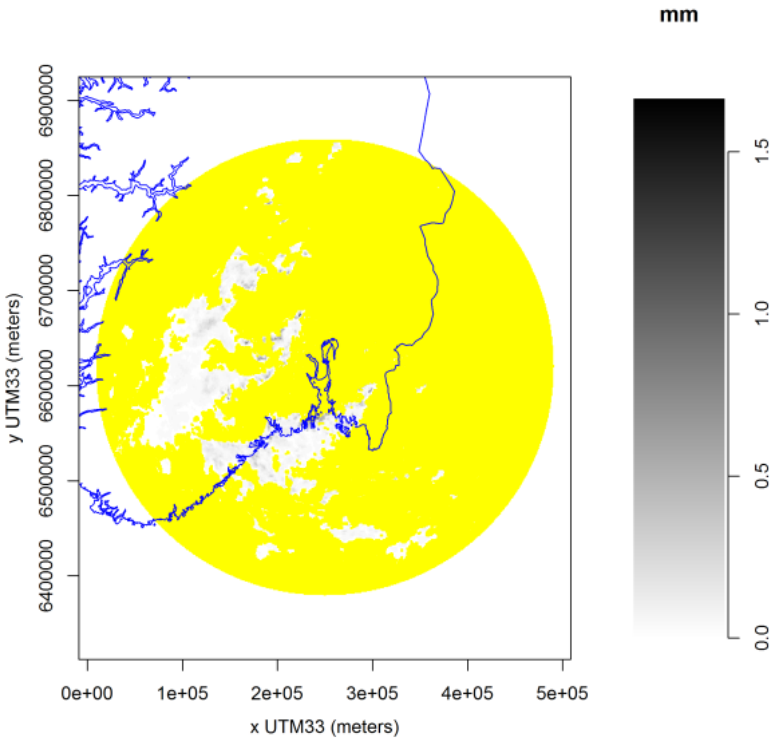
mm
y UTM33 (meters)
6900000
6800000
6700000
6600000
6500000
6400000
0e+00
1e+05
2e+05
3e+05
4e+05
5e+05
x UTM33 (meters)
1.5
1.0
0.5
0.0

a

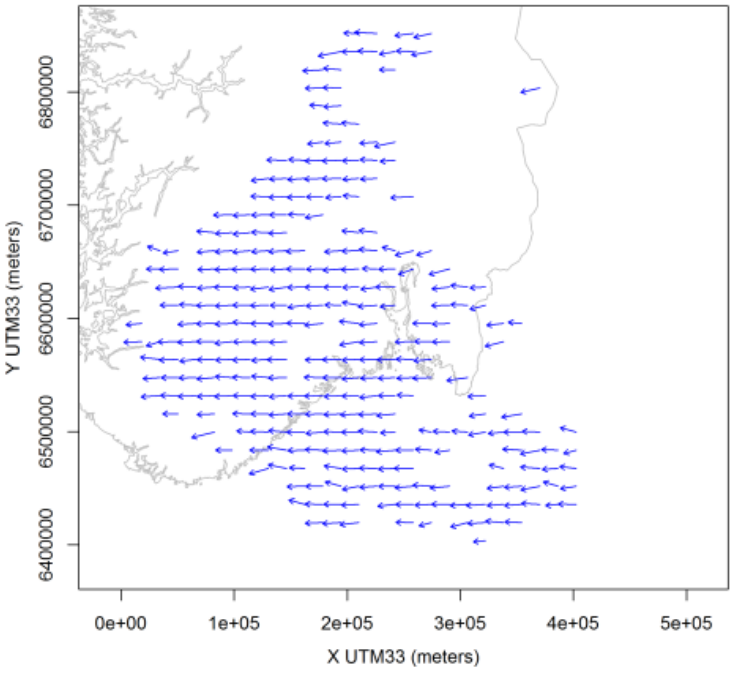
Y UTM33 (meters)
6800000
6700000
6600000
6500000
6400000
0e+00
1e+05
2e+05
3e+05
4e+05
5e+05
X UTM33 (meters)

b

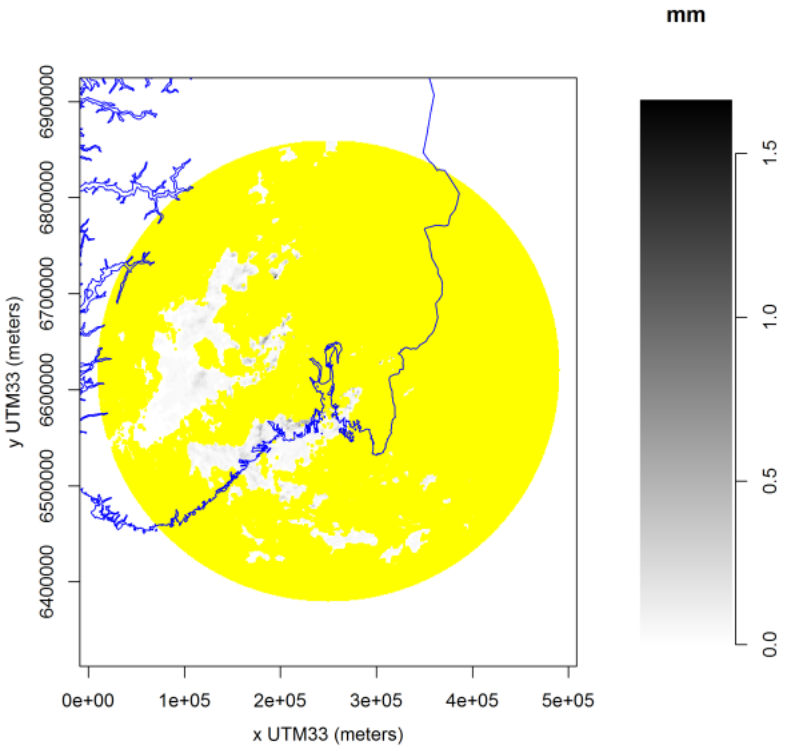
mm
1.5
1.0
0.5
0.0
y UTM33 (meters)
6900000
6800000
6700000
6600000
6500000
6400000
0e+00
1e+05
2e+05
3e+05
4e+05
5e+05
x UTM33 (meters)

c

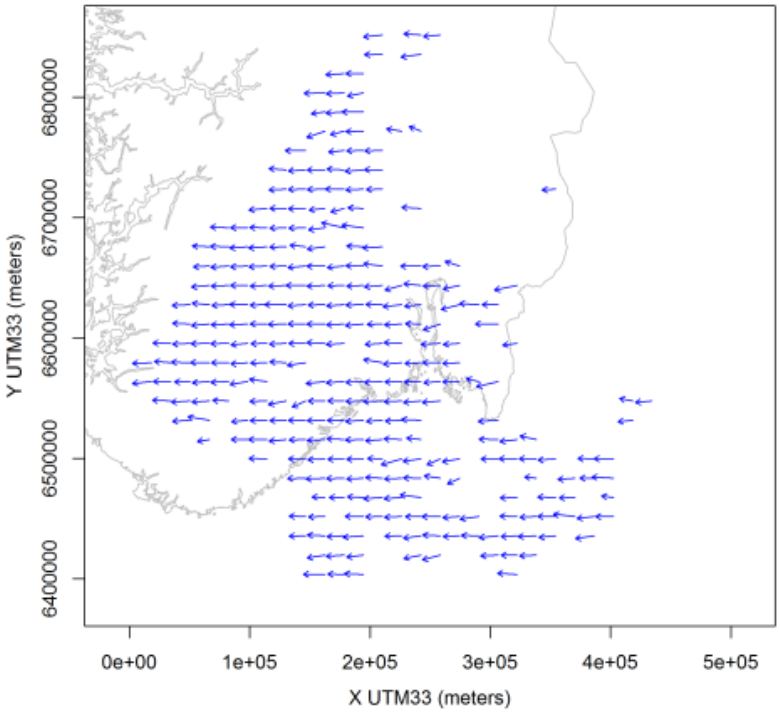
Y UTM33 (meters)
6800000
6700000
6600000
6500000
6400000
0e+00
1e+05
2e+05
3e+05
4e+05
5e+05
X UTM33 (meters)

d

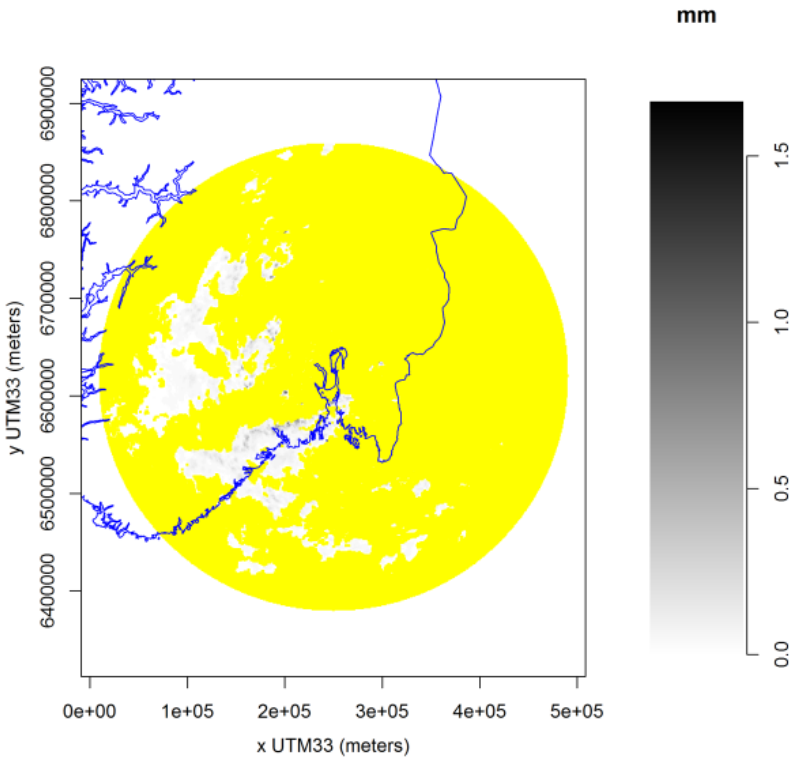
mm
y UTM33 (meters)
6400000
6500000
6600000
6700000
6800000
6900000
0e+00
1e+05
2e+05
3e+05
4e+05
5e+05
x UTM33 (meters)
0.0
0.5
1.0
1.5

e

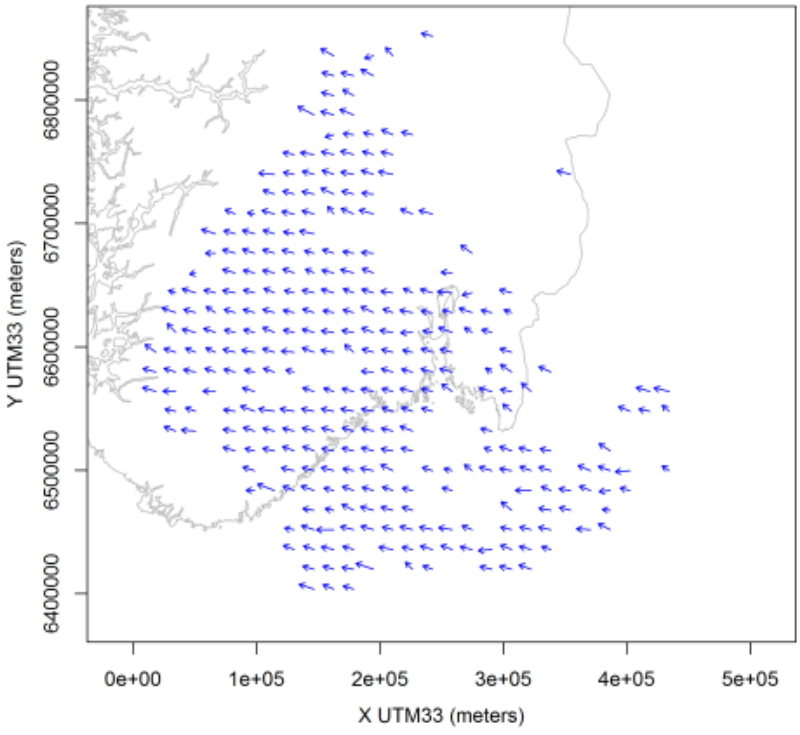
Y UTM33 (meters)
6400000
6500000
6600000
6700000
6800000
0e+00
1e+05
2e+05
3e+05
4e+05
5e+05
X UTM33 (meters)

f

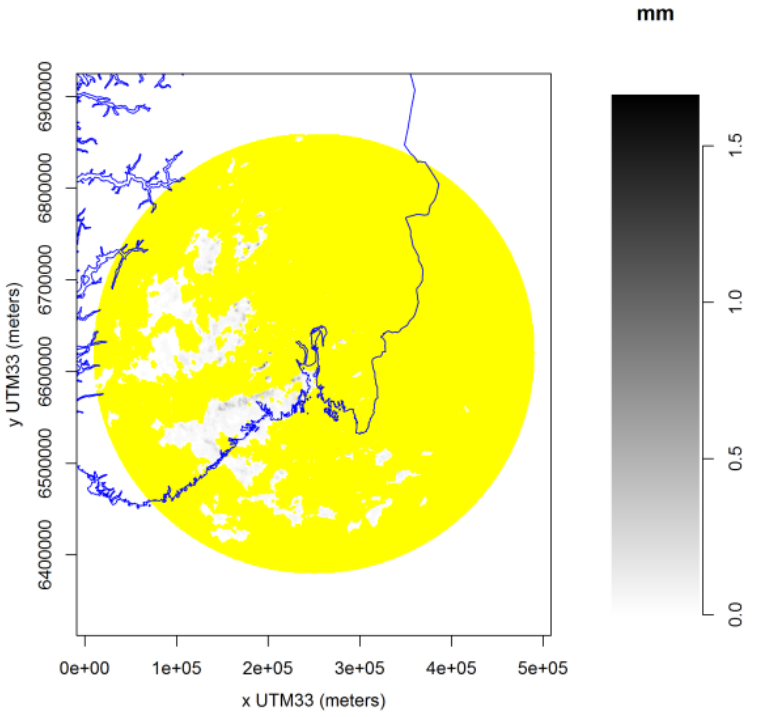


g

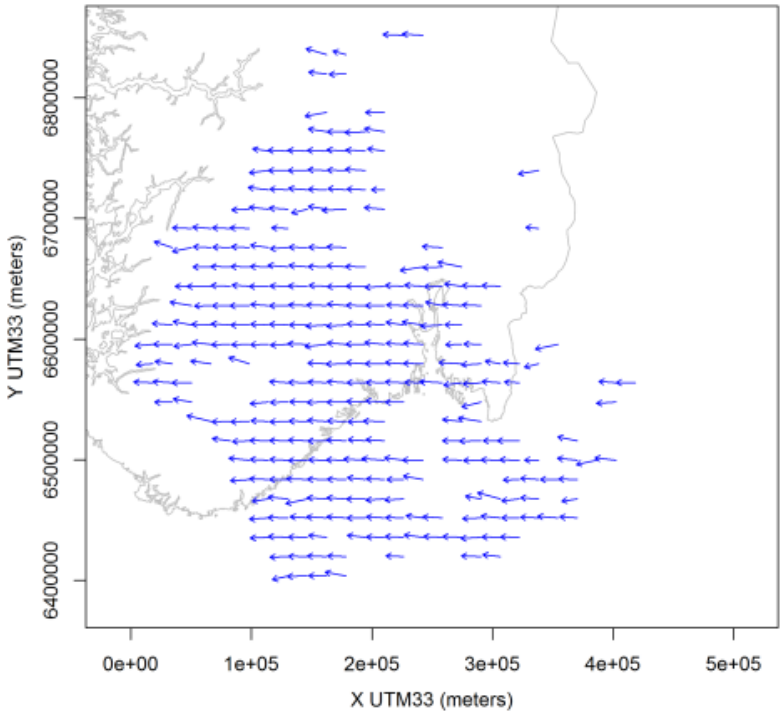


h

*Figure 16: estimated precipitation (a,c, e,g) and distributed advection (b,d,f,h) on the 23rd of July 2011 from 07:00 to 07:45*

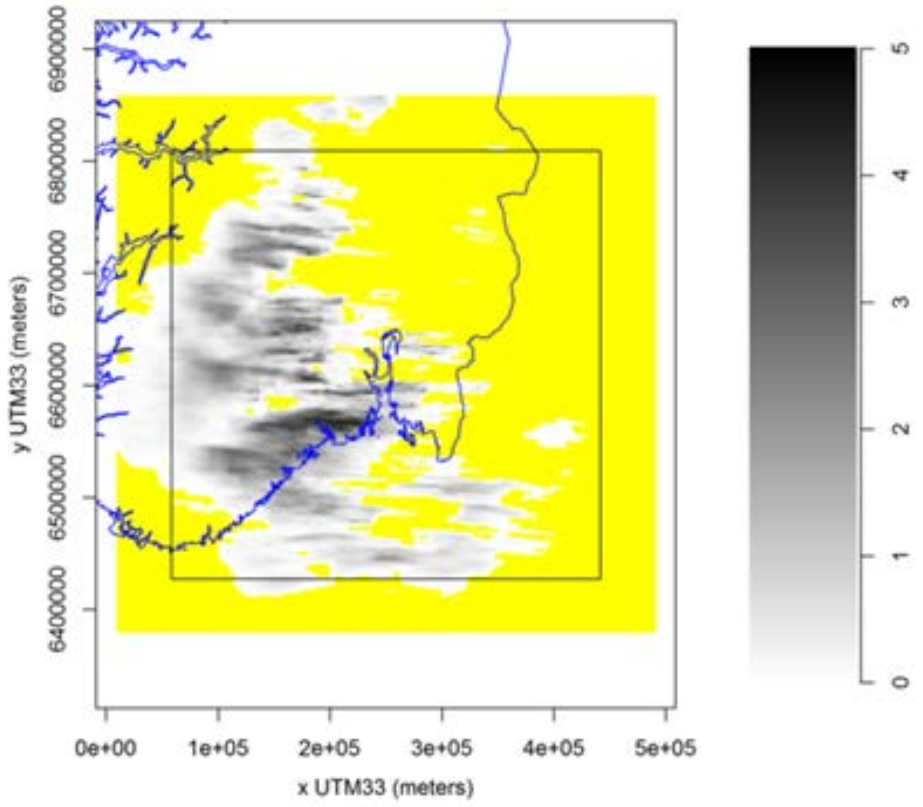


*Figure 17: Hourly aggregated precipitation on the 23rd of July 2011 from 07:00 to 07:59*

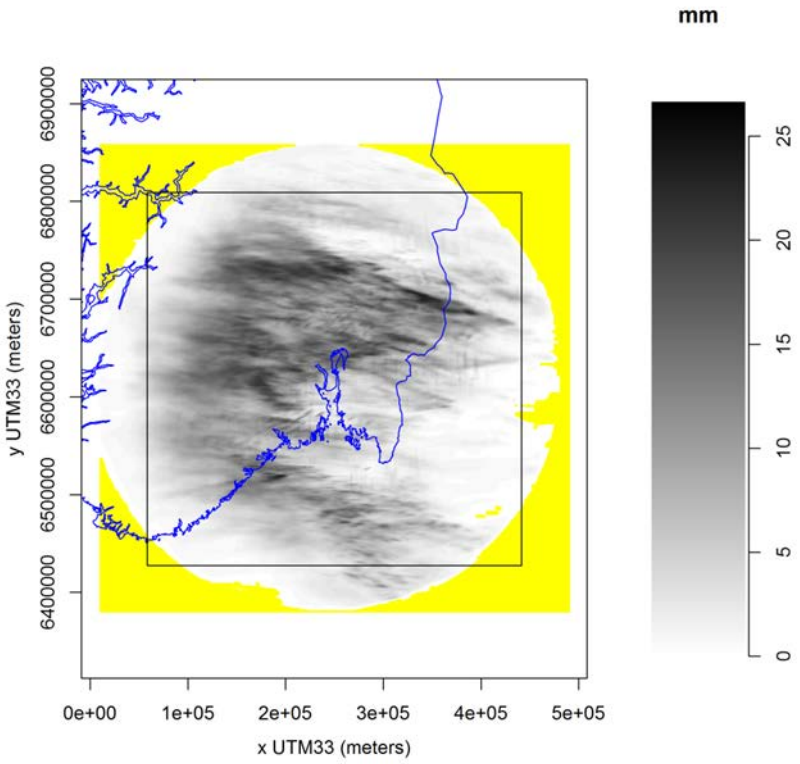


*Figure 18: Daily aggregated precipitation on the 23rd of July 2011*

## 4.3 Discussion

The temporal Lagrangian linear interpolation is a fast method to fill-in the estimated precipitation radar measured every 15minutes. It enables to increase the amount of precipitation on each pixel and to provide a realistic pattern of the precipitation field.
This method can be implemented as “on the fly” to get quickly output to be used into models belonging to a chain model.

Nonetheless the method is too coarse to retrieve a quantitatively realistic temporal structure. Moreover it does not take into account the spatial variability of the non-zero precipitation field. It does not take into account the spatial variability of the precipitation indicator field either. Figure 19 highlights this artefact. Areal mean and areal standard deviation, for the second hour of the case study event, are represented on this figure. Mean and standard deviation have been calculated for:

i-total precipitation,
ii-non-zero precipitation and
iii-precipitation occurrence.

We got measures at 0, 15, 30, 45 and 60 minutes. All the curves have a saw like behaviour. The two graphs show that the linear Lagrangian method underestimates both the areal mean

and standard deviation of the non-zero precipitation and over-estimate both the precipitation occurrence mean and standard deviation.
In other terms, the interpolation method decreases the amount of precipitation and its spatial variability and increases the size of wet area.
Aggregating the minute precipitation fields over an hour would enable to put less weight of this artefact.

Using other methods of interpolation such as Lagrangian kriging might help in keeping relevant variability and space-time structure. Nonetheless an effort would have to be done when interpolating precipitation indicator and its transition structure from dry to wet areas. This aspect is of great importance when convective precipitation phenomena occur.
Kriging is a method that assumes the field to be Gaussian. Anamorphosis, copula or other methods of conversion from a Non-Gaussian to a Gaussian field exist already. Some attention will have to be point about the correction of the structure due to this distribution transformation. Hermitian factors as described in Guillot (1999) or in Lepioufle (2009) can be applied. Superimposition of two fields: one binary field and one wet field will result as abrupt transition proper to convective. Using the GRF simulation method and filtering positive below a threshold representing the probability of intermittency (as used in Vischel et al, 2009) would not get similar characteristics. More study has to be done on that method if of use.

Using point gauges as conditioning values or as structure conditioning can be helpful.
Two approaches might be interesting:
The first is to use at-site observation as point conditioning for a radar/gage combination. However, due to its noisy behaviour, minute observation might not be the best choice as the observation to be used. Instead 10-minute, hourly and daily aggregated point values can be an alternative for the point conditioning. Combination methods such as Kalman filter and block-kriging used in Todini (1999) or Lepioufle (2012) might be interesting.
The second approach is to use a space-time stochastic simulation conditioned by point observation in order to extract the space-time structure of minutes, hourly precipitation. It provides a proxy of the pattern on location with no gauge observation. This information is then used for conditioning the structure of the interpolated the 1-minute QPE values. A Gibbs sampler might then be helpful to spread interpolated over space and time values in accordance to the proxy pattern.

QPE is an indirect measure of the radar. Spatial uncertainty will occur. An error distance must be taken into account in order to minimize this effect. Also point observations are associated with uncertainties. Point data must be checked with an efficient quality control implemented in order to filter erroneous values

Given the need related above, some specific analysis such as inner drift variogram or transition variogram must be calculated in both Eulerian and Lagrangian references. Besides some limit might appear in using usual statistics and geostatistics tools due to the size of radar data. Appendix 2 presents work and illustration on useful theory and tools on this topic.

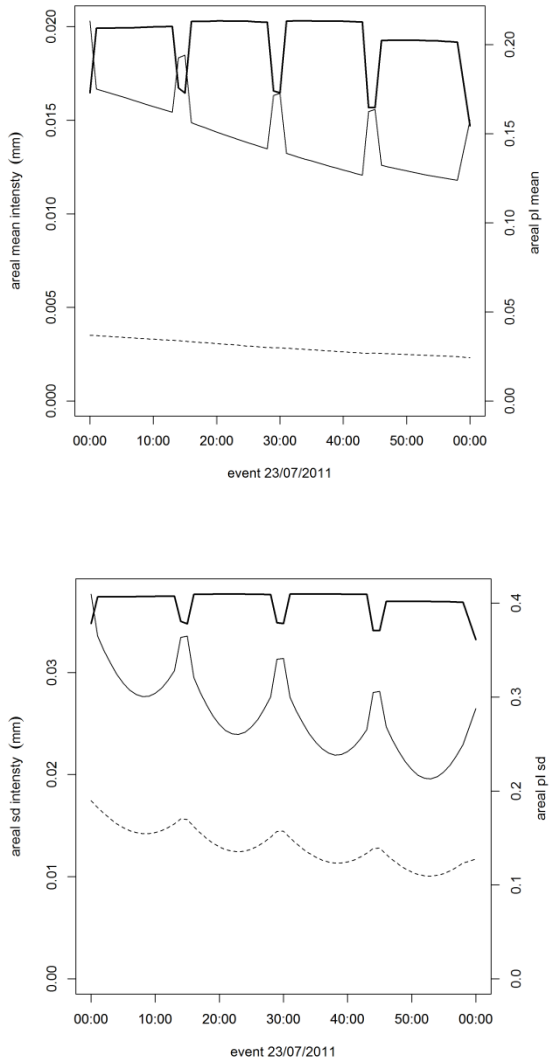


*Figure 19: Areal mean (left) and areal standard deviation (right) of minute QPE retrieved from the linear Lagrangian interpolation. Bold lines represent precipitation occurrence, thin line represent non-zero precipitation, and dashed lines represent total precipitation.*

# 5 Ensemble QPE radar

In spite of significant progress, QPE radar errors are still large and need to be taken into account, in particular in the context of operational hydrogeological applications such as issuing landslide forecast, river runoff forecasts or flash flood and debris flow warnings.

As expressed in Germann et al. (2009): "*we may think of a probability density function (pdf) that describes the range of possible values in space and time for each radar estimate. One single pdf per pixel, however, is not sufficient as errors are correlated in space and time, and one would need a pdf conditional on the values in the neighbourhood, or alternatively the full error variance–covariance matrix, the dimension of which corresponds to the total number of pixels in space and time. In practice, neither the conditional pdf nor the full error covariance matrix can be directly used in present hydrological models.*"

A promising solution to express the residual uncertainties in radar estimates is to generate an ensemble of precipitation fields, (Krajewski et al., 1985 and Germann et al., 2009). Each ensemble member is a possible realization given the reflectivity measurements and knowledge on the radar error structure (Germann et al., 2006a; Lee et al., 2007). The original (deterministic) radar precipitation field is perturbed with a stochastic component, which has the correct space–time covariance structure as defined by the radar error covariance matrix. The expression reads:

$$\phi_{t,i} = R_{R,t} + \delta_{t,i} \tag{5.1}$$

Where $R_R$ is the original unperturbed QPE radar at time t, $\delta_{t,i}$ is the perturbation field for ensemble *i* and $\phi_{t,i}$ the resulting QPE field for ensemble *i*.

The advantage of the ensemble compared to more classical approaches is the simple interface with hydrology: each member can directly be fed into the hydrological model.

The task of the ensemble generator is to model a number of realistic error perturbation fields, and to superimpose these onto the original unperturbed QPE radar field.

There is an important difference between the stochastic ensemble proposed here, and the dynamic ensemble used in numerical weather prediction models (Palmer, 2002). Here, each ensemble member is the sum of the deterministic radar precipitation field and a stochastic perturbation. The stochastic term represents the measurement uncertainty and is generated such that it has the correct space–time covariance structure as defined by the radar error covariance matrix. In the case of an ensemble system of a numerical weather prediction model, on the other hand, we have a highly nonlinear dynamic system of equations, and the initial conditions are usually perturbed such that the resulting trajectories exhibit maximum perturbation growth in phase space. The size of the ensemble is limited because of limited computing time.

## 5.1 Residual error

Assuming true precipitation known, one can write:

$$R_{TRUE} = R_R + \varepsilon \tag{5.2}$$

Where $R_{TRUE}$ represents the true QPE, $R_R$ the QPE from radar and $\varepsilon$ the error.

As written in Germann et al. (2009), most radar errors are multiplicative, it is then sensible to define the residual error ϵ in dB:

$$\varepsilon^{dB} = 10\log\left(\frac{R_{TRUE}}{R_R}\right) \tag{5.3}$$

Equation (5.2) is thus replaced by:

$$10log\ (R_{TRUE}) = 10\ log(R_R)\ +\ \varepsilon^{dB} \quad (5.4)$$

And with writing simplification:

$$R_{TRUE}^{dB} = R_R^{dB}\ +\ \varepsilon^{dB} \quad (5.5)$$

As expressed in Germann et al, 2009:

"*There are two fundamentally different approaches to characterize the parameters of the residual error in QPE radar:*

*1- Comparison with ground reference such as rain-gauge measurement* $R_G$*. This method is simple and fast and provides a direct estimate of the overall uncertainty in* $R_R$ *. The resulting parameters may overestimate the real uncertainty* $\varepsilon^{dB}$*., as the disagreement between* $R_R$ *and* $R_G$ *includes also rain-gauge and representativeness errors.*

*2- Systematic analysis of error sources. All relevant sources of residual error in* $R_R$ *are identified and quantified individually by combining measurement theory, physical concepts, sample data and statistical simulation. Second, the results of the individual error analyses are superimposed in order to determine the overall residual error parameters.*"

We chose the first option. Indeed, i-the amount of daily gauges is dense enough, ii-the study focused on one event and iii-given the topography several sources of error in QPE radar makes option 2 not obvious to established. The residual error is thus compute using the expression $10\log(R_G/R_R)$.

Daily residual error has been established using daily QPE radar and the daily manual precipitation gauges presented in the Chapter 2. Gauge measurements have been corrected following the method presented in Appendix 1 of this report.

## 5.2 Residual error estimation

Residual error in $R_R^{dB}$ are expected to be correlated both in space and time and having a Gaussian distribution. The residual reads:

$$\varepsilon^{dB} = N(\mu, \sigma, L, T) \quad (5.6)$$

Where $N$ represents a Gaussian field characterised by its mean $\mu$, its standard deviation $\sigma$, its spatial range $L$ and its temporal range $T$.

One particular case of (5.6) is the Mean Field Bias (MFB) assuming residual error invariant over space, expressed as:

$$MFB = \frac{\sum_S R_G}{\sum_S R_R} \quad (5.7)$$

Where MFB represents the ratio of the sum of values at the gauges $\sum_S R_G$ over the sum of the values of the radar pixel with gage $\sum_S R_R$

Given the complexity of the residual error structure, multivariate approach is useful. Expression (5.6) reads then:

$$\varepsilon^{dB} = \sum_i \beta_i \lambda_i + N(0, \sigma, L, T) \quad (5.8)$$

Where the $\lambda$'s correspond to covariates such as distance to the radar location (figure 20), distance to the coast (figure 21) to tell just a few, and the $\beta$'s correspond to their coefficients.

In order to have a similar approach to the Kalman filter, equations (5.6) and (5.8) have been computed with the residual error as a difference as well, i.e.:

$$\varepsilon = R_{TRUE} - R_R \qquad (5.9)$$

The restricted Maximum likelihood method has been used for the estimation of the parameters.

An algorithmic overview of the process presented in this paragraph is shown on figure 23.

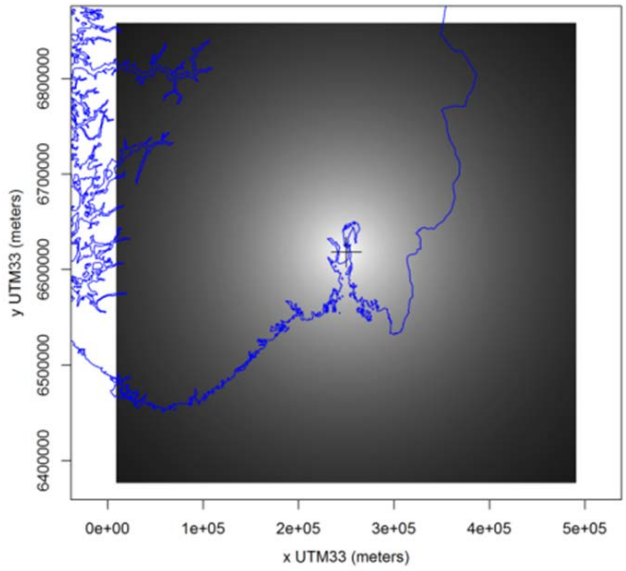


*Figure 20: Distance to the Hurum radar location*

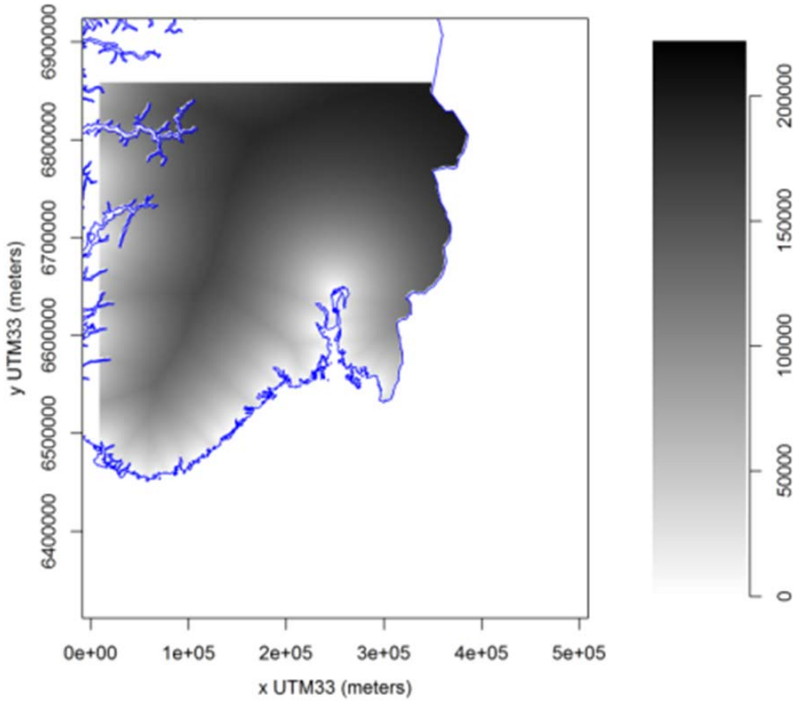


*Figure 21: Distance to the coast (meters)*

## 5.3 Ensemble QPE radar

Ensemble QPE radar at each time step is implemented by first simulating N runs of the space-time distributed Gaussian residual error expressed in (5.6) and then by superimposing it to the QPE radar in order to fulfilled expression (5.1).

Assuming a long timeseries of both radar and gage, residual error parameters are initialized once using radar–rain-gauge data from the past and are then kept constant. By doing this, parameters represent the error characteristics averaged over the selected calibration dataset.

For a real-time implementation a Bayesian approach can then be used by adding the recent residual error parameters to the a priori information i.e. the error characteristics averaged over the selected calibration dataset.

The interpolation of the residual error is an easy way to provide an “average corrected” QPE radar into hydrologic models. By using kriging as interpolation method, standard deviation of the error prediction provides the uncertainty of the output according to the error model and the gauges density.

## 5.4 Spatial classification of the daily precipitation

The multivariate linear regression error model is highly sensitive to spatial heterogeneity. Daily accumulation of convective precipitation provides such a heterogeneous field.

A clustering method has been used in order to separate the spatial field into two categories: one category of area with very high fluctuation over space and time, the second category with homogeneous precipitation. The Self-Organizing Map (SOM) approach based on Kohonen (2002) algorithm has been used for the categorization.

Variables used the for doing this categorization have been chosen in order to take into account the temporal fluctuation and the spatial fluctuation of the neighbourhood. Each pixel has been characterized by the daily coefficient of variation (i.e. ratio of the standard deviation over the mean) of non-zero precipitation for every pixel of its neighbourhood, i.e. 8 pixels.

The result is shown on figure 22.

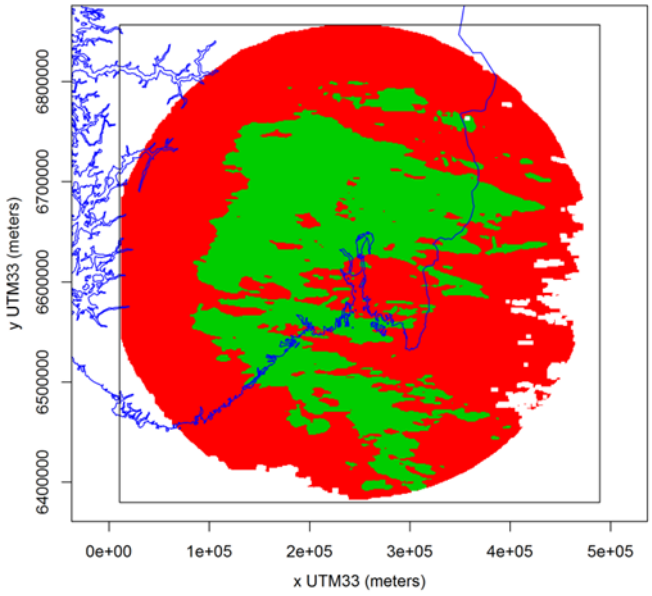


*Figure 22: footprint of precipitation over one day with: in green, very high spatial and temporal fluctuation; in red: homogeneous precipitation.*

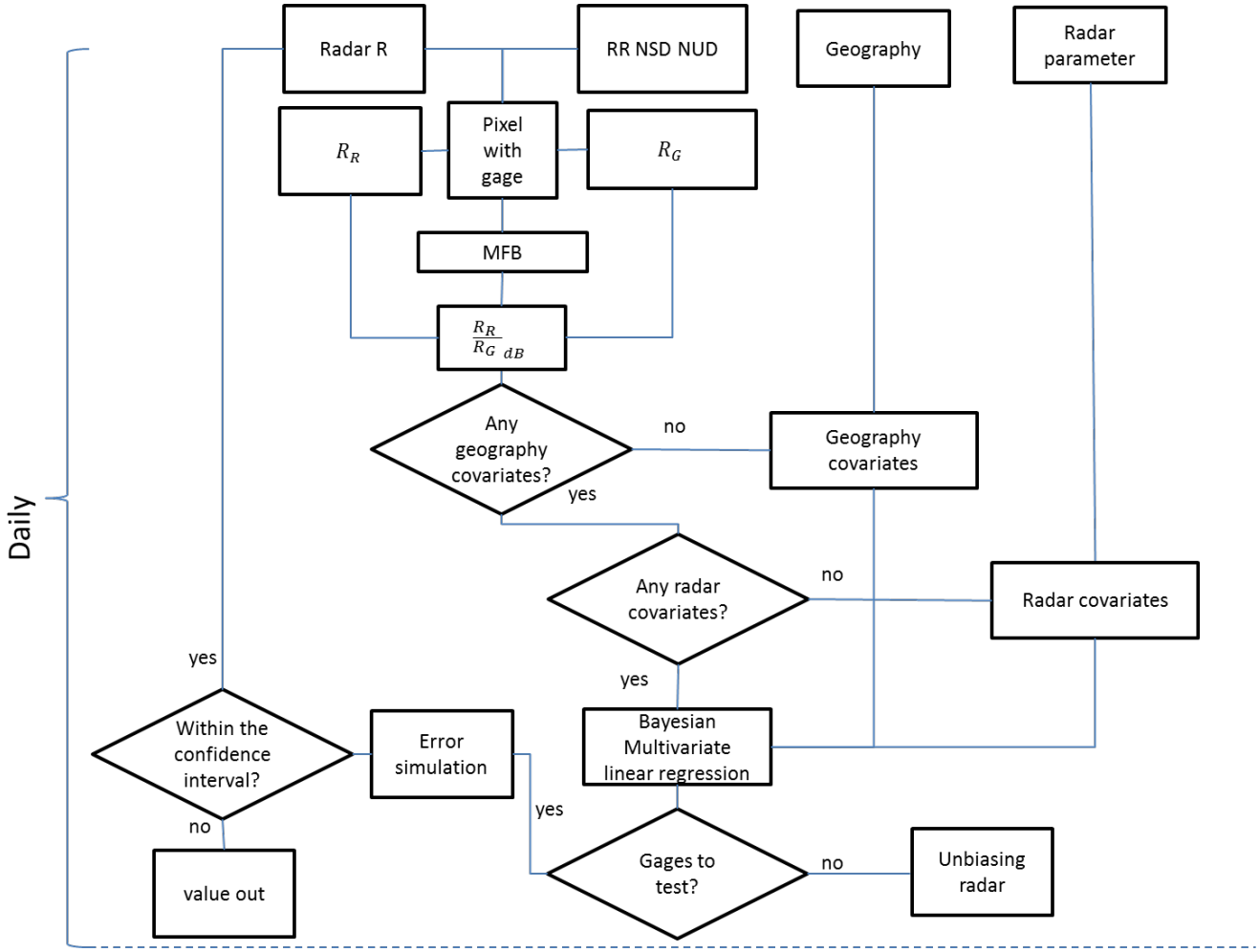


*Figure 23: Algorithmic overview of the daily QPE correction method*

## 5.5 Results

The estimation of the parameters is determined for the event of the 23rd of July 2011 for positive values of $R_R$ and $R_G$. The study is based on daily QPE. No temporal dimension has thus been taken into account. The multivariate linear model has not been used in this paragraph.

A map of the residual error on pixels with gauges highlights its distribution over space (Figure 24). The decimal logarithm has been used in order to have the ratio following a Gaussian distribution (Figure 25).

As an introduction we compared daily QPE with daily precipitation measured by gauges. No filling-in method has been used here, and measured precipitation has been assumed equivalent to a 15-min precipitation field. Figure 26 shows a quantile-quantile comparison, during the event 23rd of July 2011, of the daily gauges and the related pixel of the QPE. Values are not aligned on the black oblique line of slope 1.

The Mean Field Bias is represented on Figure 27. On the top left, a qq-plot of daily QPE and daily gauges without any correction (black) has been plotted. Corrected daily QPE using Mean Field Bias correction is shown in red colour. The top right panel represents the daily QPE with gages values described as circle proportional to the precipitation value. The bottom left panel represents the QPE after MFB correction.

The residual error has been estimated using the univariate linear model first from equation (5.6) and secondly following expression (5.9). Results are shown on figure 28 and figure 29 respectively. The top left graph represents the qq-plot of daily residual error against theoretical Gaussian values. The top right graph represents the spatial: variogram of the daily residual error. The middle left graph represents the daily QPE radar with gages values described as circle proportional to the precipitation value. The middle right graph: represents the kriged residual error. The bottom left graph represents the corrected QPE radar using the kriged residual error. The bottom right graph represents the error predication of the kriged residual error.

Bayesian approach has been implemented. Because only working on one event, no a priori information has been used. All the priori parameters $\beta_i$, $\sigma$, $L$ have been chosen following uniform distribution. Results are based on residual error expressed in (5.6) and shown in figure 30. The top left graph represents the qq-plot of daily residual error against theoretical Gaussian values, the top middle graph represents the a posteriori distribution of the average μ (intercept $\beta_0$). The top-right graph represents the a posteriori distribution of the standard deviation $\sigma$. The middle left graph represents the a posteriori distribution of the spatial range L. The middle-middle graph represents the a posteriori distribution of the nugget. The middle-right graph represents the averaged corrected QPE based on a kriged residual error with constant μ, $\sigma$, and L choose into the a posteriori distributions. The bottom-left graph represents the same as the middle-right graph with others parameters μ, $\sigma$, and L choose into the a posteriori distributions. The bottom-right graph represents one run of a Bayesian-based simulation based on non-constant μ following the a posteriori distribution, and constant $\sigma$, and L choose into the posteriori distributions.

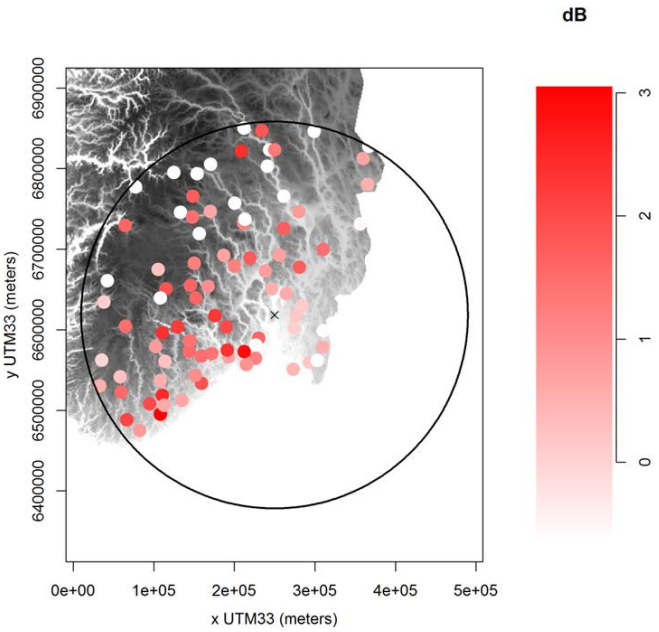


*Figure 24: Ratio daily gauge value over daily QPE on every pixel with a gauge. Unit is in dB*

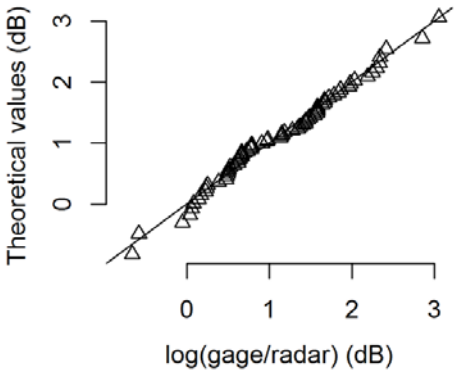


*Figure 25: Qq-plot of decimal logarithm of the ratio against theoretical Gaussian distribution*

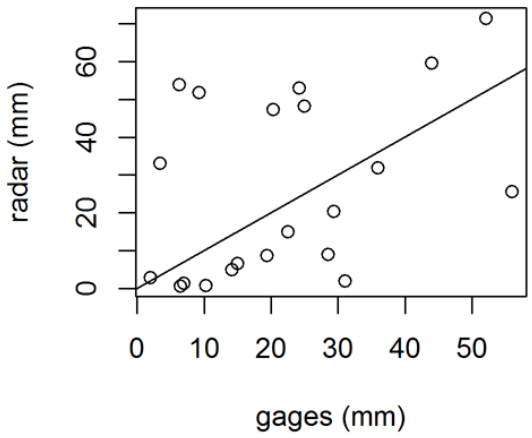


*Figure 26: Qq-plot of daily QPE and daily gauges. No filling-in method has been used here, and measured precipitation has been assumed equivalent to a 15-min precipitation field.*

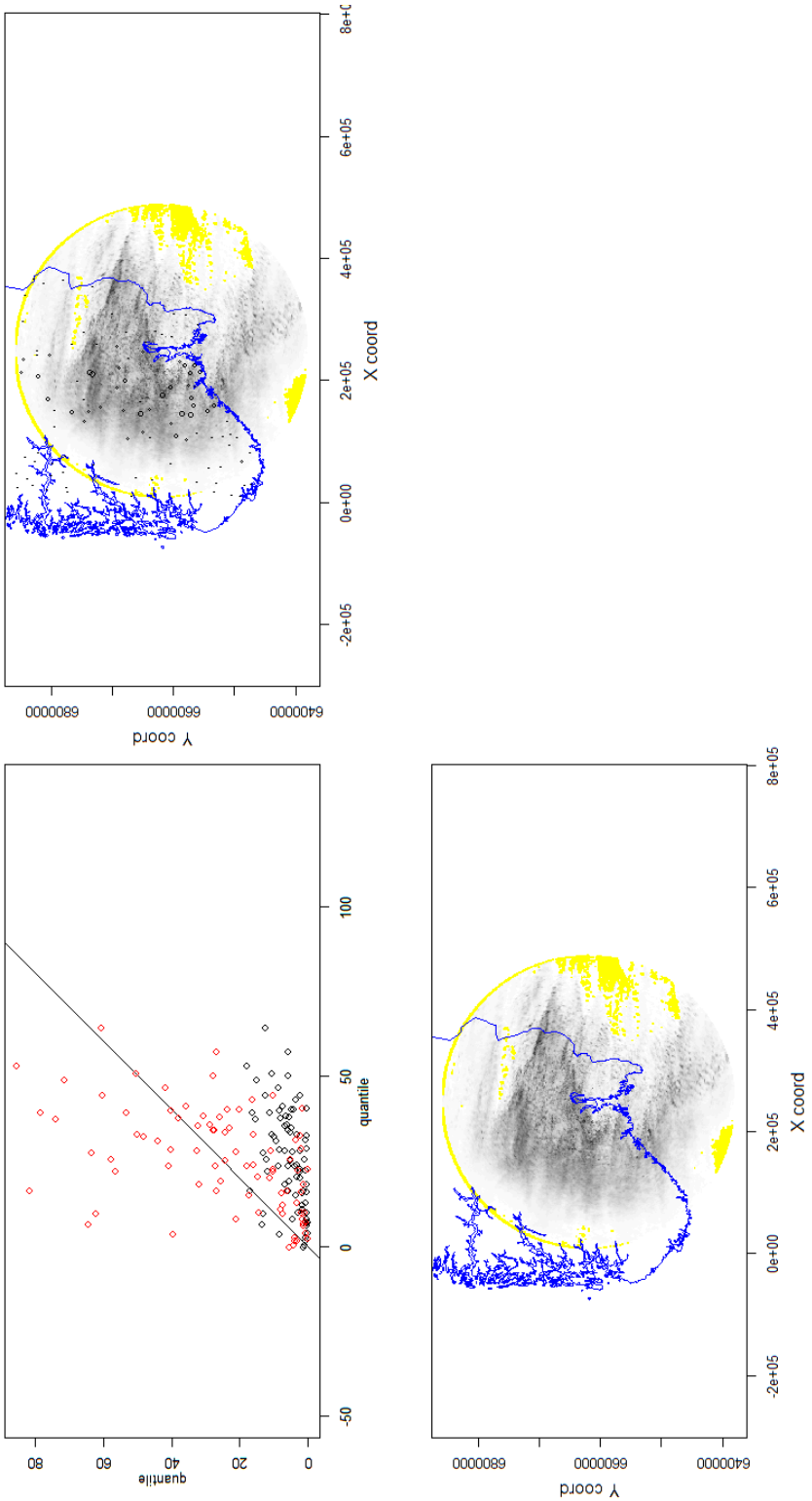


*Figure 27: Top left: Qq-plot of daily QPE and daily gauges without any correction (black), using a Mean Field Bias correction (red).Top right: daily QPE with gages values described as circle proportional to the precipitation value. Bottom left: QPE after MFB correction*

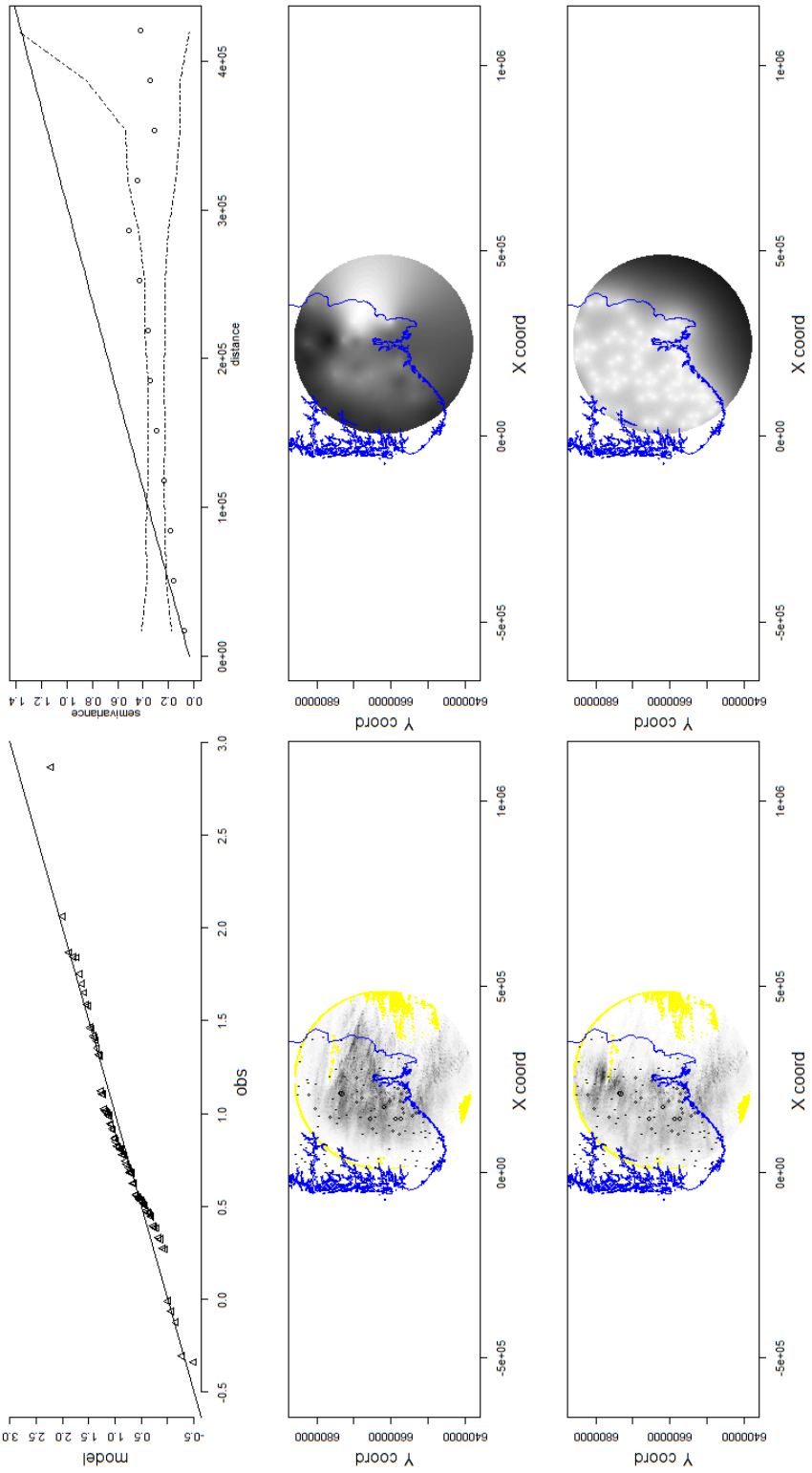


*Figure 28: Top left: Qq-plot of daily residual error against theoretical Gaussian values, Top right: spatial variogram of the daily residual error, Middle left: daily QPE with gages values described as circle proportional to the precipitation value. Middle left: kriged residual error, Bottom left: corrected QPE using the kriged residual error, Bottom right: error predication of the kriged residual error.*

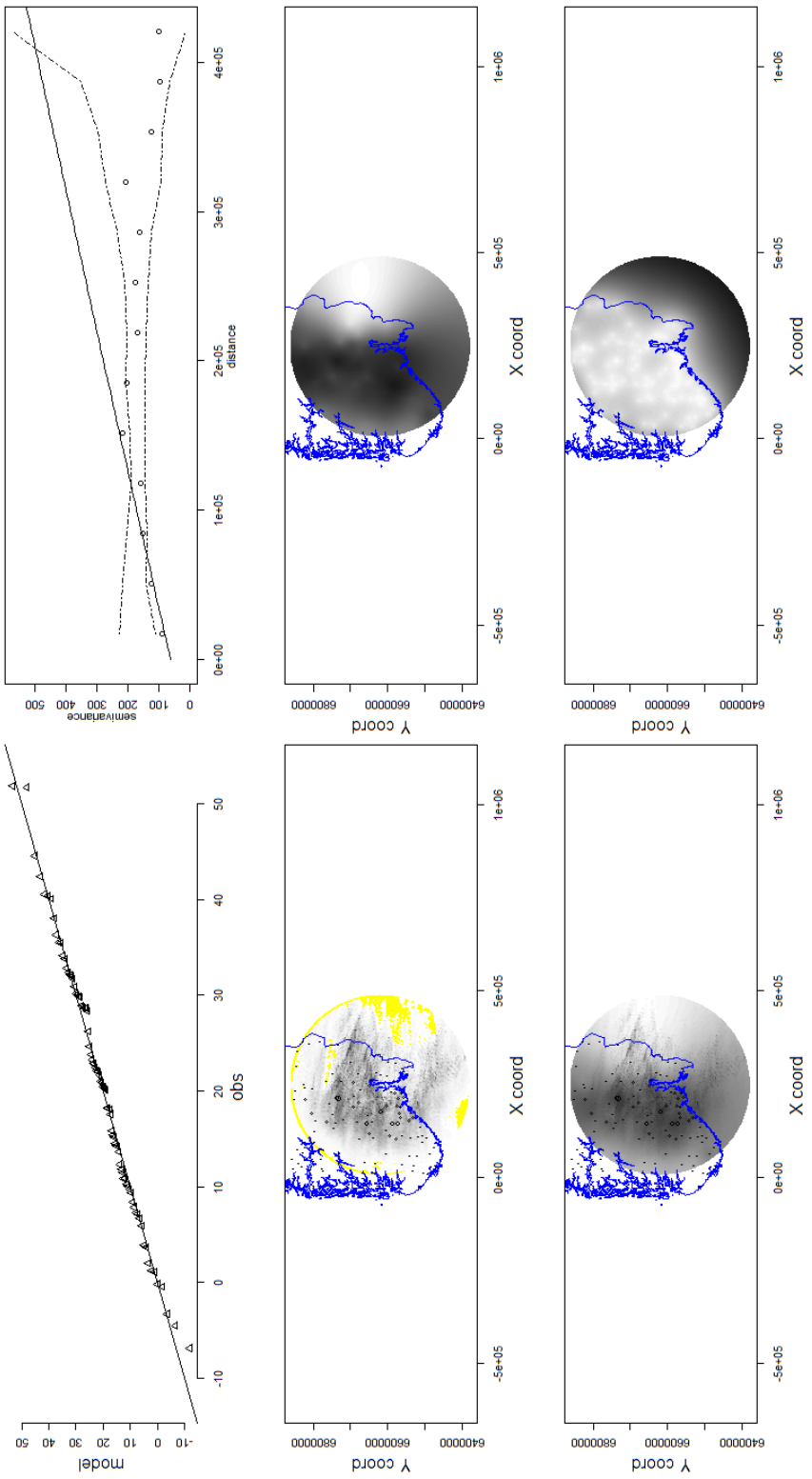


*Figure 29: Top left: Qq-plot of daily residual error against theoretical Gaussian values, Top right: spatial variogram of the daily residual error, Middle left: daily QPE with gages values described as circle proportional to the precipitation value. Middle left: kriged residual error, Bottom left: corrected QPE using the kriged residual error, Bottom right: error predication of the kriged residual error.*

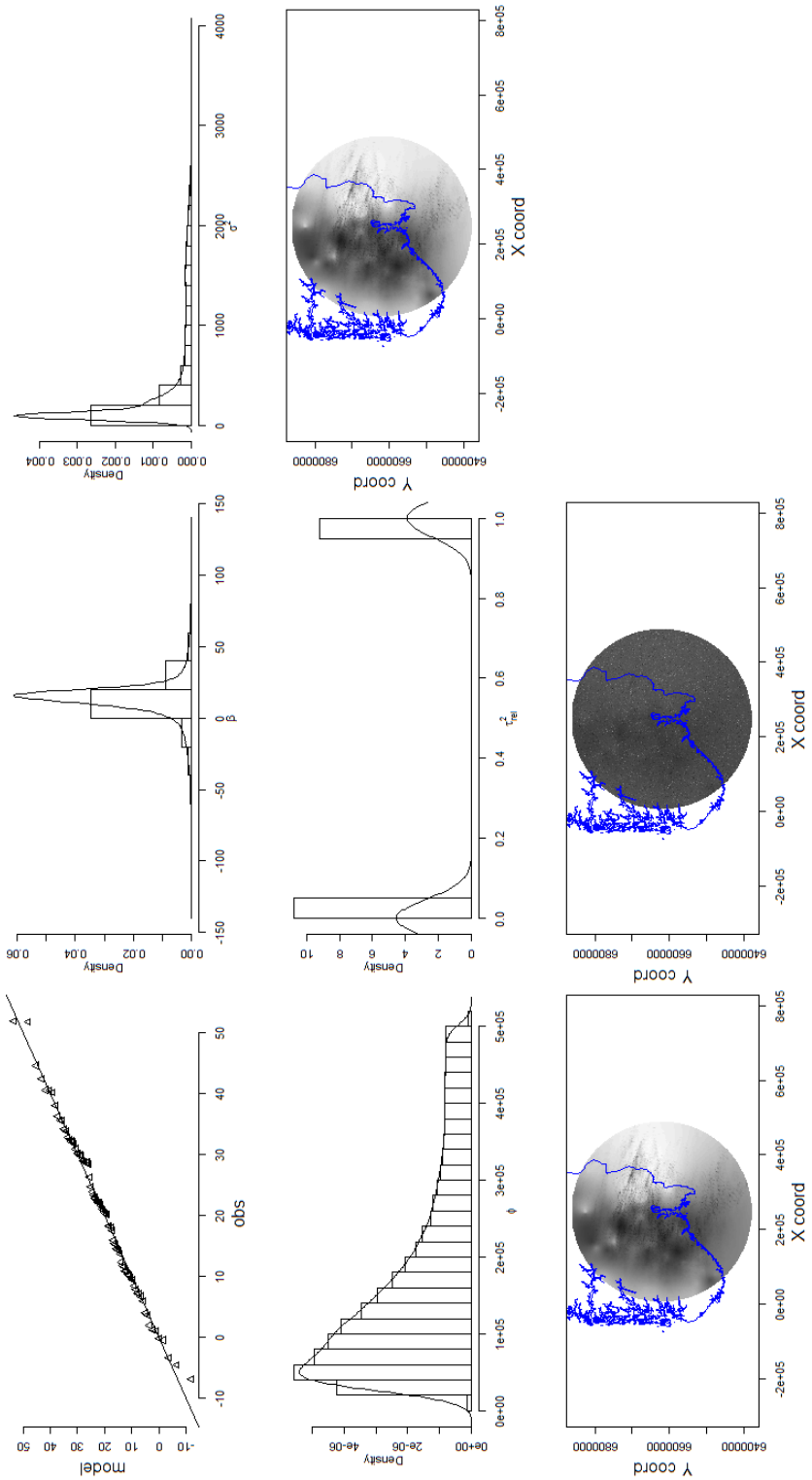


*Figure 30: Top left: Qq-plot of daily residual error against theoretical Gaussian values, Top middle: a posteriori distribution of the average μ (intercept $\beta_0$), Top-right: a posteriori distribution of the standard deviation $\sigma$, Middle left: a posteriori distribution of the spatial range L, Middle-middle: a posteriori distribution of the nugget, Middle-right: averaged corrected QPE based on a kriged residual error with constant μ, $\sigma$, and L choose into the a posteriori distributions, Bottom-left: same as middle-right with others parameters μ, $\sigma$, and L choose into the a posteriori distributions. Bottom-*

*right: one run of a Bayesian-based simulation based on non-constant $\mu$ following the a posteriori distribution, and constant $\sigma$, and L choose into the posteriori distributions.*

## 5.6 Discussion

Estimation of residual error parameters are based only on the event of the 23rd of July 2011 with the C-band radar located at Hurum.

At daily time resolution residual error, whatever taken as a ratio or a difference between gages measurements and QPE radar, follows a Gaussian distribution.

Corrected QPE radar by MFB, as shown on figure 27, does not fit to the straight line of slope 1. This method is nonetheless interesting in order to improve areal amount of precipitation over a catchment.

The averaged corrected QPE radar shown on figures 28 and 29 is similar to QPE radar/ gauges combination. It provides easily computable input into hydrologic models, landslide forecast, river runoff forecasts or flash flood and debris flow warnings. Error prediction of the averaged corrected QPE radar (figures 28 and 29) enable to get the uncertainty of the corrected values.
Attention must be taken when dealing with sub-daily difference between QPE radar and precipitation gauge measurements. A residual error based on a difference might not be Gaussian anymore.

Although results presented on figures 28 and 29 are interesting, the limited size of the dataset is not sufficient for a good estimation of the parameters. As an example, parameters of the spatial variogram (figures 28 and 29) are not correct.
More accuracy in the estimation of the parameters of residual error model can be obtained by taking into account longer timeseries or, better, several events with similar precipitation phenomena. The remark refers then to the discussion done in the Chapter 2 of this report.

Regarding the multivariate method presented in this Chapter no result has been shown. Not surprisingly, results with covariates such as distance to the coast and distance to the centre of the radar does not provide good results enough to be presented here. As said previously the short timeseries does not enable to catch the average signal of the precipitation phenomenon. Further, this convective event has been chosen because of its convective and extreme characteristics. The event is thus far away from an average convective phenomenon.

The daily time resolution did not enable the estimation a time dimension of the residual error. Sub-daily dataset timeseries will see the possibility of including a time dimension into the error model as expressed in (5.6)

Even though this chapter has been entitled “ensemble QPE, no ensemble based on the description given in paragraph 5.3 has been simulated. Nonetheless, method to get ensemble QPE radar is now known and ready to be used. Focus will now be on estimating residual error

from a long QPE radar timeseries. The simulation method is not a problem. Many R-package enable space-time simulation of Gaussian field.

A Bayesian approach has been developed in order to test adaptability to a real-time ensemble QPE. The residual error parameters estimated for the studied event has been constraint by an a priori information of the averaged signal. Given the averaged signal is unknown in our case, a uniform distribution has been used to determine the pdf's of the parameters μ, $\sigma$, and L. The implementation of a posteriori distribution is quick. A posteriori distribution provide parameter values for QPE radar simulation. Simulation outputs are highly similar to ensemble QPE. Nonetheless average behaviour of the residual error is needed in order to avoid irrelevant samples erroneously having large influence. Simulation output shown on figure 30 is an example of this case. The parameter μ value is high and characterised by a non-spatially correlated distribution. As a consequence it thus alters the whole field by producing a noisy spatial field. Instead, multivariate analysis over a long timeseries would have helped in estimating a spatially distributed trend driven by covariates.

Ungauged areas such as mountainous area might need some other work for a better accuracy of the ensemble QPE. In the absence of ground reference in such areas, one would need a simplified physical-statistical model that allows the estimate of the residual error for any given location. A systematic analysis of error sources mentioned above in Paragraph 5.1 would help substantially to construct the physical-statistical error model. Atmospheric information such as vertical instability, moisture flux convergence and other atmospheric characteristics can also be used for better modelling of the residual error.

Ensemble QPE can be used to provide input into hydrological model. In the case of urban hydrology, QPE radar must be relevant at 200m² spatial resolution, and 5 minute time resolution. C-band radar in polar reference has a non-constant spatial resolution that can be interesting in urban area next to the radar location. An X-band radar will provide data at higher spatial resolution. An adaptation of the QPE ensemble to X-band radar might then be useful.

# 6 Summary and conclusions

## 6.1 Data and case study

The whole study has been focused on the radar located at Hurum for the event that occurred on the 23rd of July 2011. A gauge network of 84 manual daily stations has been used for this study.
It has been chosen to directly transcript reflectivity into Quantitative Precipitation Estimation (QPE) using Marshall Expression with constant coefficient from literature. The reflectivity signal (*Z*) of the radar has been transformed into precipitation (*R*) using the Marshall expression $Z = aR^b$, where a=200 and b=1.6.
The uncertainties in the $Z-R$ relationships when converting $Z$ into $R$ may introduce erroneous spatial patterns of precipitation. Ideally it would have been interesting to spend time on estimating spatially distributed parameters a and b. Or more practically, to use the Marshall expression very late in the study to keep reflectivity, and thereby direct measure of radar.
An important point is the quality of the data. Statistical methods must be developed in order to know the weight to put on each value. Quality control of hourly values will need use of non-Gaussian statistics or machine learning method such as neuronal network or self-organizing map.

## 6.2 Quantitative Precipitation Nowcasting (QPN)

Quantitative Precipitation Nowcasting (QPN) is defined as very short term forecast, with a lead time from 0 hour (now) to 2 hours.
This study has focused on the feasibility of a simple nowcasting method, called Lagrangian persistence, to provide information relevant for NVE. The estimated precipitation has been assumed perfect in order to focus on the nowcasting method.
Assessment of the radar nowcasting method has been established using the SEEPS score. A degradation of performance with lead time is obvious from the figures and is expected. The spatial resolution of the nowcast has an influence on the SEEPS score. If a nowcast at pixel level does not compare well with the available observation, it does not mean that the performance is poor. In order to analyse the effect of increasing tolerance to error due to misplacement, the SEEPS was calculated for an extended verification area surrounding a nowcasted pixel. The results of the performance for larger verification area illustrates the increase in nowcast skill, as quantified by SEEPS, as the verification area is increased from a single pixel (1 km2) up to an 5 x 5 pixel area. So far the simple method does not enable to provide relevant information at the pixel resolution but enable to provide relevant spatial uncertainty information.
The QPN method used in this study can gain in improving several points:
1- The advection method
2- Growth and dissipation of precipitation
3- Precipitation nowcasting for urban hydrology
4-Convective phenomena or orographic effect modelling

## 6.3 Temporal filling-in of minute precipitation radar

Radar measurements are not continuous over time but occurred every 15 min for the event of the 23rd of July 2011 (7.5 min now). QPE radar does not represent a temporal accumulation over 15 min. Indeed the frequency of measurement is different from the measure resolution. As a consequence zebra pattern appears when aggregating over time. We assumed that estimated precipitation from radar to be a 1-min time resolution measurement. Filling-in the estimated

precipitation between every 15 min time step make the estimated precipitation field more realistic.
The temporal Lagrangian linear interpolation is a fast method to fill-in the estimated precipitation radar measured every 15 minutes. It enables to increase the amount of precipitation on each pixel and to provide a realistic pattern of the precipitation field.
This method can be implemented as “on the fly” to get quickly output to be used into models belonging to a chain model.
Nonetheless is the method too coarse to retrieve a quantitatively realistic temporal structure. Moreover it does not take into account the spatial variability of the non-zero precipitation field. It does not take into account the spatial variability of the precipitation indicator field either.
Using other methods of interpolation such as Lagrangian kriging might help in keeping relevant variability and space-time structure. Nonetheless an effort would have to be done when interpolating precipitation indicator and its transition structure from dry to wet areas. This aspect is of great importance when convective precipitation phenomena occur.

## 6.4 Ensemble QPE radar

In spite of significant progress, QPE radar errors are still large and need to be taken into account, in particular in the context of operational hydrogeological applications such as issuing landslide forecast, river runoff forecasts or flash flood and debris flow warnings.
The task of the ensemble generator is to model a number of realistic error perturbation fields, and to superimpose these onto the original unperturbed QPE radar field.
The advantage of the ensemble as opposed to more classical approaches is the simple interface with hydrology: each member can directly be fed into the hydrological model.
At daily time resolution residual error, whatever taken as a ratio or a difference between gauges measurements and QPE radar, follows a Gaussian distribution.
Applying corrected QPE radar by the easy method MFB is interesting for improving areal amount of precipitation over small catchment for example
The interpolation of the residual error is an easy way to provide an “average corrected” QPE radar into hydrologic models and is similar to radar/gages combination. By using kriging as interpolation method, standard deviation of the error prediction provides the uncertainty of the output according to the error model and the gauges density. The averaged corrected QPE radar provides easily computable input into hydrologic models, landslide forecast, river runoff forecasts or flash flood and debris flow warnings.
Attention must be taken when dealing with sub-daily difference between QPE radar and precipitation gauge measurements. A residual error based on a difference might not be Gaussian anymore.
More accuracy in the estimation of the parameters of residual error model will be reached by taking into account longer timeseries or, better, several events with similar precipitation phenomena.
Regarding the multivariate method presented in this Chapter 5 no result has been shown. Not surprisingly, results with covariates such as distance to the coast and distance to the centre of the radar have not provide good results enough to be presented here. As said previously the short timeseries does not enable to catch the average signal of the precipitation phenomenon. Further, this convective event has been chosen because of its convective and extreme characteristics. The event is thus far away from an average convective phenomenon.
Even though the chapter has been entitled “ensemble QPE, no ensemble based on the description given in paragraph 5.3 has been simulated. Nonetheless, method to get ensemble QPE radar is now known and ready to be used. Focus will be done now on estimating residual

error from a long QPE radar timeseries. Simulation method is not a problem. Many R-package enable space-time simulation of Gaussian field.
A Bayesian approach has been developed in order to test adaptability to a real-time ensemble QPE. The residual error parameters estimated for the studied event has been constraint by an a priori information of the averaged signal. Given the averaged signal unknown in our case, uniform distribution has been used to determine the pdf's of the parameters μ, $\sigma$, and L. Implementation of a posteriori distribution is quick. A posteriori distributions provide set of parameter values for QPE radar simulation. Simulation outputs are highly similar to ensemble QPE. Nonetheless average behaviour of the residual error is of need in order to avoid irrelevant samples erroneously having large influence. Simulation output shown on figure 30 is an example of this case. The parameter μ value is high and characterised by a non-spatially correlated distribution. It thus alters the whole field by producing, as a consequence, a noisy spatial field. Instead, multivariate analysis over a long timeseries would have helped in estimating a spatially distributed trend driven by covariates.
Ungauged areas such as mountainous area might need some other work for a better accuracy of the ensemble QPE. In the absence of ground reference in such areas, one would need a simplified physical-statistical model that allows the estimate of the residual error for any given location. A systematic analysis of error sources mentioned in Paragraph 5.1 would help substantially to construct the physical-statistical error model. Atmospheric information such as vertical instability, moisture flux convergence and other atmospheric characteristics must be used for a better modelling of the residual error.

## 6.5 Conclusion

The report presents methods and examples to provide QPN and ensemble QPE radar. Tools have been developed for an easy access, and further developments (Appendix 3).
Further work can be focused on using longer timeseries of QPE radar at sub-daily time resolution.

Simple operational tools can be built easily in the next few years for the whole Norway.
More attention would have to be put on areas with no reference sensor such as mountainous areas. Physic-statistic model based on the physics of the radar will be of a great help for these cases. Description of convective events might gain from these physic-statistic models as well.
Analyses of the extremes and of the Intensity/duration/Area/frequency can gain of the ensemble QPE.

Incorporating ensemble QPE into a hydrologic model or landslide model will enable to analyze the propagation of the uncertainties through chain models. The chain can first be applied for hindcasting and then for forecasting (Rossa et al, 2011).

A robust Bayesian framework can be settled by following Renard et al. (2011).

# 7 References


Abdella, Y.S., Tøfte, L.S, (2013) A preliminary investigation of the potential of radar-based short-term precipitation forecasting in central Norway An experiment on using Lagrangian persistence for nowcasting of two events. SINTEF TR A7379

Allen, R. J., and A. T. DeGaetano (2005), Considerations for the use of radar-derived precipitation estimates in determining return intervals for extreme areal precipitation amounts, J. Hydrol., 315, 203, doi:10.1016/j.jhydrol.2005.03.028.

Amani, A. Lebel. T. (1997 Lagrangian kriging for the estimation of Sahelian rainfall at small time steps Journal of Hydrology - J HYDROL , vol. 192, no. 1, pp. 125-157

Austin PM. 1987. Relation between measured radar reflectivity and surface rainfall. Mon. Weather Rev. 115: 1053–1070.

Barancourt, C. Etude de l'intermittence et de la variabilité des champs de precipitation par une approche stohastique, thesis for docteur-ingénieur, 271 pp, Univ Joseph Fourrier Grenoble 1, 1990

Barancourt, C.  Creutin, JD Rivoirard, J. (1992) A method for delineating and estimating rainfall fields

Bellon A, Lee G, Kilambi A, Zawadzki I. (2007). Real-time comparisons of VPR-corrected daily rainfall estimates with a gauge mesonet. J. Appl. Meteorol. 46: 726–741.

Berenguer M, Corral C, Sanchez-Diezma R, Sempere-Torres D. 2005. Hydrological validation of a radar-based nowcasting technique. J. Hydrometeorol. 6: 532–549.

Bowler NE, Pierce CE, Seed AW. (2006). STEPS: A probabilistic precipitation forecasting scheme which merges an extrapolation nowcast with downscaled NWP. Q. J. R. Meteorol. Soc. 132: 2127–2155

Delrieu G, Andrieu H, Creutin JD. 2000. Quantification of path integrated attenuation for X- and C-band weather radar systems operating in Mediterranean heavy rainfall. J. Appl. Meteorol. 39: 840–850.

Durrans, S. R., L. T. Julian, and M. Yekta (2002), Estimation of depth-area relationships using radar-rainfall data, J. Hydrol. Eng., 7, 356 – 367

Dyrrdal, A.V. (2012), Estimation of extreme precipitation in Norway and a summary of the state-of-the-art, MET report no 08/2012

Elo, C.A., (2012), Correcting and quantifying radar data, MET report no 2/2012

Førland, E.J. (red), P. Allerup, B. Dahlström, E. Elomaa, T. Jónsson, H. Madsen, J. Perälä, P. Rissanen, H. Vedin and F. Vejen (1996), Manual for operational correction of Nordic precipitation data, DNMI KLIMA Report 24/96

Germann U. 1999. Radome attenuation – A serious limiting factor for quantitative radar measurements? Meteorol. Z. 8: 85–90.

Germann, U., Berenguer, M., Sempere-Torres, D., Zappa, M., (2009) REAL—Ensemble radar precipitation estimation for hydrology in a mountainous region. doi: 10.1002/qj.375

Germann U, Joss J. 2002. Mesobeta profiles to extrapolate radar precipitation measurements above the Alps to the ground level. J. Appl. Meteorol. 41: 542–557.

Germann, U. and I. Zawadzki (2002), Scale-Dependence of the Predictability of Precipitation from Continental Radar Images. Part I: Description of the Methodology. Mon. Wea. Rev., 130, 2859–2873.

Germann U, Zawadzki I. (2004). Scale-dependence of the predictability of precipitation from continental radar images. Part II: Probability forecasts. J. Appl. Meteorol. 43: 74–89.

Germann U, Zawadzki I. 2006. Predictability of precipitation from continental radar images. Part IV: Limits to prediction. J. Atmos. Sci. 63: 2092–2108.

Guillot, G.,(1999) Approximation of Sahelian rainfall fields with meta-Gaussian random functions Part1: model definition and methodology, Stochastic Environmental Research and Risk Assessment 13

Joss J, Gorieg, EG. 1978. Shapes of raindrop size distributions. J. Appl. Meteorol. 17: 1054–1061.

Joss J, Lee R. 1995. The application of radar-gauge comparisons to operational precipitation profile corrections. J. Appl. Meteorol. 34: 2612–2630.

Joss J, Waldvogel A. 1990. Precipitation measurement and hydrology. Pp 577–597 in Radar in Meteorology: Battan Memorial and 40$^{th}$ Anniversary Radar Meteorology Conference. Amer. Meteorol. Soc: Boston.

Kitchen M. 1995. 'Estimation of surface precipitation rate from radar using a variational method'. Pp 228–238 in COST-75Weather Radar Systems – International Seminar, Brussels 1994 vol. EUR 16 013 EN.

Krajewski WF, Georgakakos KP. 1985. Synthesis of radar rainfall data. Water Resour. Res. 21: 764–768.

Lee G-W, Zawadzki I. 2005. Variability of drop size distributions: Time-scale dependence of the variability and its effects on rain estimation. J. Appl. Meteorol. 44: 241–255.

Lepioufle, JM., Modélisation spatio-temporelle d'un champ de pluie; Application aux pluies journalières du bassin versant de la Loire, PhD thesis, Institut National Polytechnique de Grenoble, Cemagref, Lyon, p. 162. 2009

Lepioufle, JM. Leblois, E. Creutin, JD. (2012) Variography of rainfall accumulation in presence of advection, Journal of Hydrology 464–465 494–504

Lepioufle, JM., Radar data combined with raingauges method, SINTEF report, 2012

Li, L., W. Schmid, and J. Joss (1995), Nowcasting of motion and growth of precipitation with radar over a complex orography, J. Appl. Meteorol., 34, 1286–1300

Yonggang Liu and Robert H. Weisberg (2011). A Review of Self-Organizing Map Applications in Meteorology and Oceanography, Self-Organizing Maps - Applications and Novel Algorithm Design, Dr Josphat Igadwa Mwasiagi (Ed.), ISBN: 978-953-307-546-4, InTech

Lombardo, F., F. Napolitano, and F. Russo (2006), On the use of radar reflectivity for estimation of the areal reduction factor, Nat. Hazards Earth Syst. Sci., 6, 377 – 386.

Mohr M. New Routines for Gridding of Temperature and Precipitation Observations for "seNorge.no", MET report No. 08/2008

Overeem, A., T. A. Buishand, and I. Holleman (2009), Extreme rainfall analysis and estimation of depth-durationfrequency curves using weather radar, Water Resour. Res., 45, W10424, doi:10.1029/2009WR007869

Pellarin T, Delrieu G, Saulnier G-M, Andrieu H, Vignal B, Creutin J-D. 2002. Hydrologic visibility of weather radar systems operating in mountainous regions: Case study for the Ard`eche catchment (France). J. Hydrometeorol. 3: 539–555.

Renard, B., Kavetski,B., Leblois, E., Thyer, M., Kuczera, G., Franks, S.W., (2011) Toward a reliable decomposition of predictive uncertainty in hydrological modeling: Characterizing rainfall errors using conditional simulation, WATER RESOURCES RESEARCH, VOL. 47, W11516, doi:10.1029/2011WR010643

Mark J. Rodwell, David S. Richardson, Tim D. Hewson and Thomas Haiden, (2010) A new equitable score suitable for verifying precipitation in numerical weather prediction, Q. J. R.Meteorol. Soc. 136: 1344–1363, Part A

Ødemark, K., Førland, E., Mamen, J., Elo, C.A., Dyrrdal, A.V., Myrabø, S., (2012), Ekstrem korttidsnedbør på Østlandet fra pluviometer og radar data, MET report no 78/2012

Rossa, A., Liechti, K., Zappa, M., Bruen, M., Germann, U., Haase, G., Keil, C., Krahe, P.,(2011) Uncertainty Propagation in Advanced Hydro-Meteorological Forecast Systems, Volume 100, Issues 2–3, Pages 150–167

Seed AW. 2003. A dynamic and spatial scaling approach to advection forecasting. J. Appl. Meteorol. 42: 381–388.

Todini, E., (2001) A Bayesian technique for conditioning radar precipitation estimates to rain-gauge measurements, Hydrology and Earth System Sciences, 5(2), 187–199

Tveito, O. E., E. Førland, R. heino, I. Hansen-Bauer, H. Alexandersson, B. Dahlström, A. Drebs, C. Kern-Hansen, T. Jónsson, E. Vaarby Laursen and Y. Westman, (2000),Nordic temperature maps, MET Report no. 09/00

Tveito, O. E., I. Bjørdal, A. O. Skjelvåg and B. Aune (2005) A GIS-based agro-ecological decision system based on gridded climatology, Met. Apps., Vol. 12: 1, p. 57-68, 2005

Vischel, T., et al. (2009) Conditional simulation schemes of rain fields and their application to rainfall–runoff modeling studies in the Sahel. J. Hydrol. doi:10.1016/j.jhydrol.2009.02.028

Wolff, M. Isaksen, K., Ødemark, K., Petersen-Øverleif, A., Reitan, T. og Brækkan, R., Vindkorreksjon av nedbør, et Energi Norge prosjekt, MET report 22/2013

Yang, Y., X. Chen, and Y. Qi (2013), Classification of convective/stratiform echoes in radar reflectivity observations using a fuzzy logic algorithm, J. Geophys. Res. Atmos. 118, 1896–1905, doi:10.1002/jgrd.50214.

Zawadzki I. 1982. The quantitative interpretation of weather radar measurements. Atmos.–Ocean 20: 158–180.

# Appendix 1: Daily correction of manual precipitation gauges

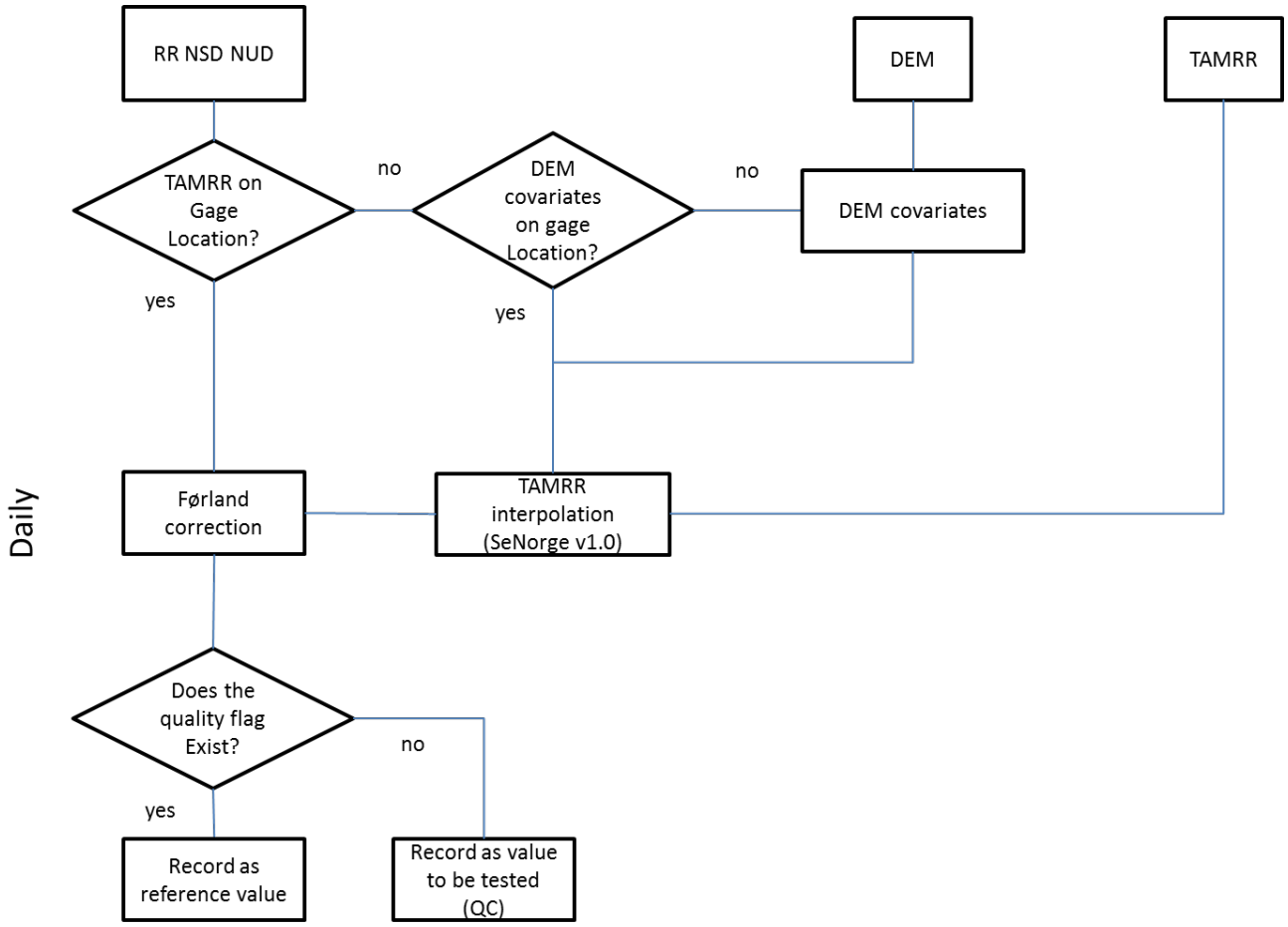


*Figure A1.1: Algorithmic sum-up of the daily precipitation correction method for manual gauges*

# Appendix 2: Geostatistics modelling and tools

Statistic and geostatistic tools have been developed in order to get all needed information for analysis, modelling, interpolation and simulation. Codes enable omni-directional and directional analysis of spatial fields on regular or irregular grids. Variogram, co and cross-variograms enable the study of fields like non-zero precipitation, precipitation occurrence, inner drift variability and transition variability following Barancourt (1990, 1992) and Lepioufle (2009) for the modelling of various precipitation phenomena as convective or stratiform.
Appendix 2 presents a synthesis of useful theory.
Illustrations will be presented in the tutorial reports.

## Precipitation space-time structure

Spatial structure of QPE is expressed as a variogram,

$$\gamma(h) = \frac{1}{2} E\left[\left(Z(x) - Z(x+h)\right)^2\right] \quad \text{(A2.1)}$$

Where *Z* represents a random variable at the space-time location *x*

According to Lepioufle (2009) and following Barancourt, 1990, the variogram for precipitation field can be decomposed into variogram of precipitation intermittency ($\gamma_I$), variogram of non-zero precipitation ($\gamma_F$) and the transition variogram $\gamma_{Tr}$:

$$\gamma(h) = \left({m_I}^2 - \gamma_I(h)\right).\gamma_F(h) + 2\gamma_I(h).\gamma_{Tr}(h) \quad \text{(A2.2)}$$

## Intermittency

Intermittency characterized the presence or absence of precipitation. It results in a binary variable where *I* = 1 for *Z* > 0 and *I* = 0 for *Z* = 0. The intermittency variogram indicates the length of wet areas. Sample variogram is calculated as:

$$g_I(h) = \frac{1}{2n}\sum_{i=1}^{n}\left(I_i(x) - I_i(x+h)\right)^2 \quad \text{(A2.3)}$$

The variance of the precipitation intermittency is given as $\sigma_I^2 = m_I(1 - m_I)$ where $m_I$ is the probability of having precipitation..

## Inner variability

The variogram of the non-zero precipitation describes the inner variability and is calculated as:

$$g_F(h) = \frac{1}{2n_F}\sum_{i=1}^{n_F}\Big(F_i\ (x) - F_i\ (x+h)\Big)^2 \quad \text{(A2.4)}$$

where $F$ is the precipitation values were z > 0. The variance of the precipitation is given as $\sigma_F^2$

## Transition dry/wet areas

The transition variogram describes the smoothness of transition from dry to wet areas and is calculated as:

$$g_{Tr}(h) = \frac{1}{2n_{Tr}}\sum_{i=1}^{n_{Tr}}\Big(F_i\ (x) - I_i^0(x+h)\Big)^2 \quad \text{(A2.5)}$$

where $I^0$ is the binary data where *I*=0.

The dependency between intermittency and inner variability is of importance when modelling precipitation.
Barancourt (1990), then Barancourt et al (1992) highlights the importance of investigating the inner drift, i.e. the shape of precipitation values within wet areas. The inner drift is expressed as:

$$\gamma_{ZI}(h)/\gamma_I(h) \quad \text{(A2.6)}$$

In the case where the shape of precipitation within wet area is constant, then the inner drift is equal to $m_F$.

Barancourt (1990), then Lepioufle (2009) highlights the importance of investigating the transition from between wet areas to dry areas:

$$\gamma_{Tr}(h) = \frac{1}{2}\gamma_{Z^2I}(h)/\gamma_I(h) \quad \text{(A2.7)}$$

In the case where transition between dry and wet area is abrupt, the transition is equal to $({m_F}^2 + {\sigma_F}^2)/2$.

## Use of this theory overview

Results based on Appendix2.1 to Appendix2.3 enable to provide parameters for interpolation or simulation.
Results in Appendix2.4 enable to know the error as the consequence of a superposition of a field *F* with a field *I*. In case of a non-convective phenomenon, the transition will be smooth. The transition variogram gives an indicator of the temporal aggregation you need to apply on your assume elemental structure to get a realistic variogram that represents this phenomena.
Non-stationary methods and temporal aggregation methods of original model should enable to pass by some potential artefact.
This theory can be used for both space and time dimension. In the case of a temporal analysis, it is important to work in the Lagrangian reference in order to catch the dissipation fluctuation. In

Eulerian reference, fluctuation can appear lower because of a ration fluctuation/advection (Lepioufle, 2012) to low.

In order to compute sample variogram and their estimation on big size fields, sub-sampling of the fields, with respect of the wet/non-wet area ratio, has been applied. This method provides robust results with low cpu demanding. This subsampling method is used among other at MeteoSwiss.

# Appendix 3: Tools development

All the tools applied in this feasibility study have been developed under R. Open-source R-packages have been developed to be used for the different tasks presented in this report (figure A3.1). All of these R-packages will be put on GitHub for a free use. For an easy use of these packages and in order to ease a continuous development of the R-packages, "holding R-packages", scripts and procedures have been created (figure A3.2).

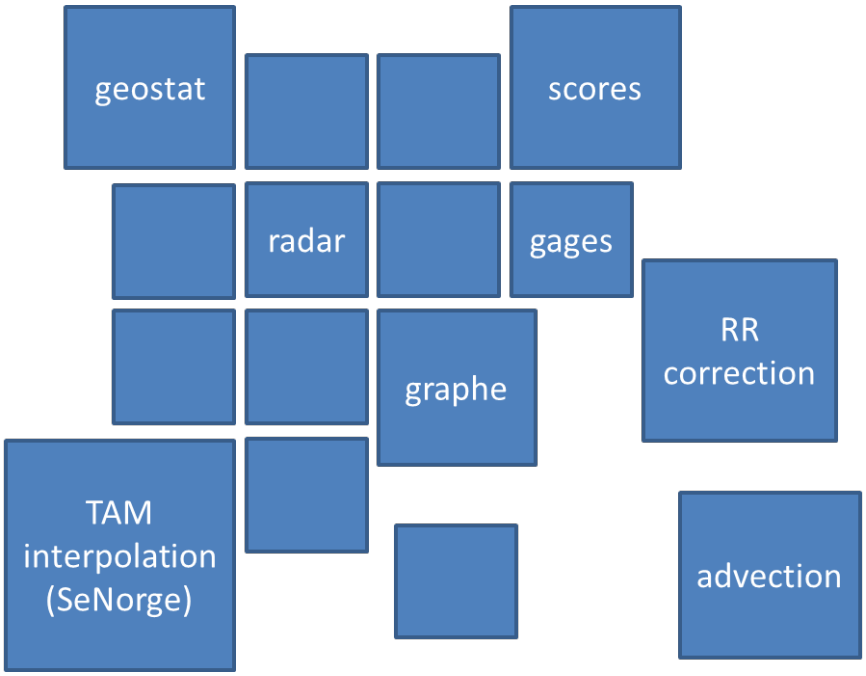


*Figure A3.1: illustration of R-packages developed for this project*

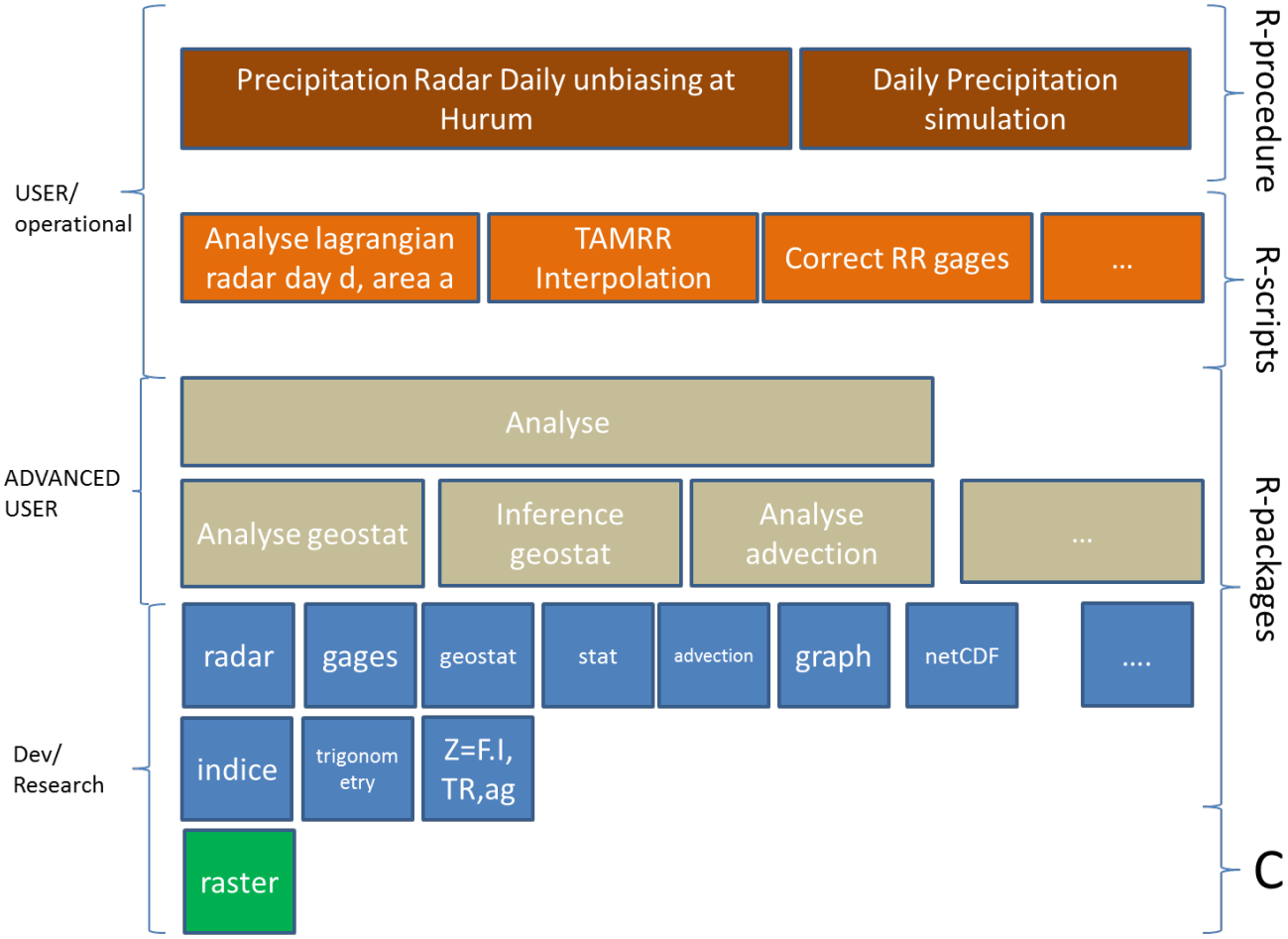


*FigureA3.2: architecture of the packages, scripts and procedures according to the need of the users*